Higher harmonic wave exciting forces
on a vertical cylinder

by

J. Grue, G. Bjørshol and Ø. Strand

Higher harmonic wave exciting forces
on a vertical cylinder

by John Grue, Gunnhild Bjørshol and Øyvind Strand

Department of Mathematics, Mechanics Division
University of Oslo, Norway

An experimental study of the loads due to long waves on a restrained vertical circular cylinder is presented. The wave height is varied from a small value up a value being comparable to the cylinder diameter. A higher harmonic oscillation becomes present in the recorded force when the wave height exceeds a certain value. The higher harmonic oscillation occurs about one quarter wave period after the main peak in the loading. It starts when the wave crest is about one cylinder radius behind the cylinder's rear and reaches a maximum when the wave crest is about one cylinder diameter behind the cylinder's rear. It then decays to zero. The higher harmonic force oscillation lasts for about 15% of the wave period, has a magnitude up to 11% of the peak-to-peak value of the total force and has a resultant acting approximately one cylinder radius below the mean water line. The experiments indicate that this is a suction force, and that its presence is governed by the Froude number based on the particle velocity at the wave crest, the cylinder diameter and the acceleration due to gravity. The higher harmonic force appears in measurements when the Froude number equals 0.35 and becomes pronounced for Froude numbers exceeding 0.4.

1   Introduction

Wave exciting loads generating high frequency ringing responses of offshore structures is a current important problem within offshore technology. Ringing responses are experienced at the resonance frequencies of monotower gravity-based platforms and tension-leg platforms, the former being a platform placed on a vertical cylinder extending down to the sea floor, the latter with a submerged part being constructed by vertical cylinders placed on a pontoon. The ringing responses of these platforms are experienced for high sea-states. A typical wave length is then longer than about ten times the cylinder diameters and the wave height is comparable to the cylinder diameters.

In this contribution we consider laboratory measurements of the wave loads acting on one restrained vertical cylinder. The experiments are carried out in a wave tank. The ratios

of the wave length and the wave height to the cylinder diameter are in the experiments about 13 and up to 1.2, respectively, being relevant for the large scale conditions where the ringing responses of the platforms are experienced.

The wave loading due to a transient wave group is considered. We adopt a wave generation similar to that described by Dommermuth et al. (1988). A positive interference between the wave group's components then creates a high leading wave of the wave group at the position of the cylinder. Working with a transient wave group is found to be of advantage in a wave tank with limited breadth. The main events in the present experiments then occur before reflections from the tank walls are disturbing the flow at the cylinder. The main results of the experiments are, however, also believed to be valid when the incident waves is a regular wave train of constant amplitude in an open sea condition, or in a broad wave tank where the reflections from the tank walls are very limited.

In the present experiments the wave height is varied between a lowest value up to a largest value leading to a plunging breaker. For small wave height the wave loads are found to be well predicted by the inertia term of Morison's equation. By increasing the wave height the recorded forces become skewed. In addition, a secondary oscillation appears in the force recordings. The secondary oscillation occurs about one quarter wave period after the main peak in the loading. It starts when the wave crest is about one cylinder radius behind the cylinder's rear and reaches a maximum when the wave crest is about one cylinder diameter behind the cylinder's rear. It lasts for about 15% of the wave period, has a magnitude up to 11% of the peak-to-peak value of the total force and has a resultant acting approximately one cylinder radius below the mean water line. Simultaneous recordings of the free surface behind the cylinder reveal a considerable low-pressure taking place behind the cylinder during the same time period as the secondary force oscillations occur, indicating that this secondary force oscillation is a suction force.

When the wave height is small, the local fluid accelerations determine the wave forces. A non-dimensional number characterizing the fluid accelerations is the wave number multiplied by the cylinder diameter. If the wave height is large compared to the cylinder diameter, the value of the Keulegan-Carpenter number becomes an important parameter. There is, however, another non-dimensional number which is of importance to the present problem. Our results indicate that the particle velocity under the wave crest is an important parameter in the experiments. Furthermore, the force recordings indicate that the secondary force oscillation is due to a free surface effect, i.e. the effect due to gravity. A non-dimensional particle velocity is then given by the Froude number based on the cylinder diameter. In fact, the appearance of the secondary force oscillation occurs with a pronounced effect when the Froude number equals 0.4. For this value of the Froude number the forced wave due to a local current with velocity equal to the particle velocity at the wave crest equals the cylinder diameter. A resonance between the free surface and the body may then take place, creating a skewness in the problem, giving rise to a suction force.

Earlier experimental studies of wave loads in high sea-states have considered only the steepest waves. A recent reference is Zhou, Chan and Melville (1991) who consider wave impact pressures on vertical cylinders. In that paper a review of the literature concerning forces due to extreme waves may be found. Theoretical studies of nonlinear higher harmonic

wave loads on vertical cylinders are basically due to second order theory (Eatock-Taylor and Hung 1987, Kim and Yue 1989, Chau and Eatock-Taylor 1992). Second order theory is, however, believed to not be relevant for phenomenons being revealed in the present contribution.

In section 2 the experimental set up and procedure is discussed. The measurements of the forces and the free surface elevation are presented in sections 3 and 4, respectively. Section 5 is a discussion of the findings.

2 Experimental set up and procedure

The experiments are carried out in a wave tank at Department of Mathematics, University of Oslo. The wave tank is 14.2m long, 0.47m broad and is filled with water at a depth 0.42m. The tank is at one end equipped with a wave maker being a vertical rigid plate. The wave maker is driven by a hydraulic servo-controlled cylinder which can perform horizontal motions under program control. The wave generation is very accurate and repeatable. At the other end of the tank there is a 1.5m long absorbing beach, which reflects less than 10% of the crest height of the incoming waves. In the present experiments, however, the interesting events occur long before the incoming waves have arrived at the beach.

A circular cylinder made of plexiglas is used in the experiments. The cylinder's height is 69.5cm, the diameter is 11.9cm. The draught is 41.1cm, which means that the cylinder extends amost to the bottom of the wave tank except for a clearance of 0.9cm. The cylinder axis is located at the wave tank's centerplane, with a distance 564.3cm from the average position of the wave maker's front.

The forces are recorded by two Hottinger Baldwin Messtechnik Type Z6C2 force transducers. The maximum load is 100N (Newton), the natural frequency is 340Hz. The rise time is 7ms, and the phase delay of the forcetransducer/amplifier is 10ms, being much shorter time intervals than the rise times of the recorded forces. The sampling frequency is 100Hz. The cylinder is mounted to one force transducer at a location $Z_u = 27.5cm$ above, and to one force transducer at a location $Z_l = 36cm$ below the mean water line. The transducers are fixed to a vertical beam extending downwards from an arrangement above the wave tank. The horizontal force component along the wave tank direction is recorded.

The cylinder/beam arrangement has a natural frequency of 18.5Hz. This resonance is excited in some of the experiments introducing horizontal accelerations of the cylinder/beam. The resonant accelerations are larger at the lower force transducer than at the upper, indicating that the resonant cylinder motions are basicly pitching vibrations. The resonant excitation occurs at one time instant in three of the experiments, and at two time instants in one experiment, giving rise to resonant oscilliations in the force histories being of almost constant amplitude for succeeding time. Thus, the force transduers record the actual forces with constant horizontal accelerations of the cylinder/beam multiplied by the total mass superposed. The resonance period is, however, well below the dominant periods of the wave loading in the experiments, and it is therefore appropriate to filter out the oscillations at the natural frequency to obtain the actual forces.

The force transducers are static calibrated. The accuracy of the force recording arrangement is tested by measuring the forces due to low-amplitude regular incoming waves with wave period $O(1s)$. The recorded forces are then compared with predictions by linear theory, showing a very good agreement. In fact, the discrepancies between the measured forces and the theoretical predictions are found to be within the accuracy of the recordings of the incoming wave elevation, which is 5%. The present experiments are very repeatable. We have also demounted the cylinder several times to recalibrate the force transducers. Repeated force recordings show a very small relative scatter, being at most 5 − 10%, even in the most extreme cases.

The surface elevation is recorded by four wavegauges with a resolution of about 0.1mm. The force and wave recordings are simultaneous. The gauges are static calibrated. The accuracy of the analog-to-digital recording of the free surface elevation is tested by mounting the gauges to a motorized eccentric which forces the gauges to perform a harmonic vertical oscillation of given amplitude in calm fluid, to simulate the recording of oscillatory wave motion. Repeated tests with this arrangement revealed that the recording of the surface elevation has a relative accuracy always better than 5%. The wave recording procedure is also documented by Grue (1992). Utilizing the repeatability in the present experiments we may change the location of the wave gauges from run to run and still record the same wave field. We are thus able to make approximately simultaneous recordings of the surface elevation at several locations in the wave tank.

2.1   The wave characteristics

The wave maker is programmed to generate a transient wave group with positive interference creating a large wave height at the cylinder position. The applied wave maker displacements are based upon the results described by Dommermuth et al. (1988) who consider plunging breaking waves. In the present experiments we shall, however, vary the height of the generated waves from a lowest value being in the regime of linear wave theory and up to a largest height leading to a plunging breaker. This is done by adjusting the wave maker amplitude by a constant factor α, which is varied between $\alpha = 0.224$ and $\alpha = 1$. At $\alpha = 1$ a plunging wave is generated, with reentry occurring $41cm$ behind the location of the cylinder axis. At $\alpha = 0.875$ a spilling wave is created, with the spilling event occurring $26 - 41cm$ behind the location of the cylinder axis. The time history $X(t)$ of the wave maker's diplacements is shown in figure 1 for $\alpha = 1$. The frequency range is $0.65Hz < f < 1.3Hz$, with a center frequency being $0.98Hz$.

The resulting waves at the cylinder position are mainly characterized by the crest height, ζ_{max}, the wave height, H, and the wave length, λ, as indicated in figure 2. Additional wave parameters like e.g. skewness parameters of the waves may be relevant to the problem, but are believed to very little influence the main results. Eight different cases, A - H, of the incident wave group are considered. The wave parameters at the cylinder position are listed in table 1 for each of the cases. The local wave slope, which may be estimated by $\epsilon = K\eta_{max}$, where $K = 2\pi/\lambda$ denotes the wave number, varies in the present experiments between 0.07 and 0.34. In the case H this estimate is somewhat conservative.

In all the cases A - H the main wave crest arrives at the position of the cylinder axis

4

case	α	λ	ζ_{max}	H	$K\zeta_{max}$
A	0.224	144cm	13mm	22mm	.06
B	0.485	151cm	35mm	53mm	.15
C	0.612	155cm	50mm	74mm	.20
D	0.680	157cm	60mm	87mm	.24
E	0.749	158cm	70mm	100mm	.28
F	0.812	162cm	80mm	117mm	.31
G	0.875	164cm	90mm	129mm	.34
H	1	165cm	90mm	141mm	.34

Table 1: Wave characteristics, cases $A - H$. α denotes the constant amplitude factor for the time history of the wave maker. The wave characteristics of the incident wave group at the location of the cylinder axis are: ζ_{max}: the measured local crest height, H: the measured local wave height, λ: the measured local wave length, $K\zeta_{max}$: the local wave slope ($K = 2\pi/\lambda$).

for $t \simeq 11.4s - 11.6s$. First we consider one case, viz. case E. The time record of the surface elevation, ζ_0, at the position of the cylinder axis is shown for this case in figure 3a for a longer time interval, i.e. $9s < t < 14s$. We note that the maximum of ζ_0 occurs at $t = t_m \simeq 11.6s$. The local wave period at the cylinder position, P, may be estimated by the period between two successive zero up-crossings of the elevation occurring right before and right after $t = t_m$. For case E we find that the zero up-crossing period is $P \simeq 1.00s$. Time records of ζ_0 are then shown in figures 3b-f for the cases B, C, E, G, H, for the time interval $11s < t < 12.4s$. The zero up-crossing period in these examples is always found to be $P \simeq 1.00s$, except in case H where P is slightly larger.

In Case A, which is within the regime of linear wave theory, the local wave length and wave period must obey the linear dispersion relation for gravity waves. By applying as wave period $P = 1.00s$, we find $\lambda = 148cm$. This is consistent with the measured wave length in case A within a relative discrepancy of 2.7%, which is below the relative accuracy in the experiments. Table 1 reveal that the wave length increases with increasing wave steepness. This increase is in accordance with the dispersion relation for weakly nonlinear gravity waves.

3   The force measurements

The time histories of the forces recorded by the upper and lower force transducers are then considered. The interest is focused on the time interval when the first longer wave crest is passing the cylinder position, i.e. the time interval $11.2s < t < 12.2s$, see figures 3a-f. The force histories within this time interval are displayed in figures 4b-h. The force histories in case E are shown in figure 4a during a longer time interval for completeness. We note that the magnitude of the recorded force at the lower forcetransducer is always larger than at

the upper.

First the cases B and C are considered, with the results shown in figures 4b and 4c, respectively. In these examples the force histories are, practically speaking, found to be proportional to the recorded values of $\partial \zeta_0 / \partial t$ of the incident wave group at the cylinder position. This is an expected result. For waves with small wave slope we have that the horizontal velocity, U_0, is proportional to the surface elevation, ζ_0. This means that $\partial U_0 / \partial t$ is proportional to $\partial \zeta_0 / \partial t$. In other words, we obtain that the recorded force on the cylinder is proportional to the horizontal fluid acceleration of the incident wave group, $\partial U_0 / \partial t$, measured at the cylinder axis (with the cylinder absent). This is in accordance with the inertia term in Morison's equation which may be applied when the wave height is small and the incoming wave is long compared to the cylinder diameter. In fact, by taking into account the exponential decay in $\partial U_0 / \partial t$ along the vertical coordinate, we may evaluate the force on the cylinder from Morison's equation using the recorded values of ζ_0. This procedure shows good agreement with the measurements in case B. In case C this procedure is more crude. The effect of the limited breadth of the the wave tank leads to a 5% increase of the cylinder's added mass. This is accounted for in the evaluations of the inertia term in Morison's equation.

We then consider the cases D – H. The wave height is now increased, leading to changes in the force curves. One change is that the force curves become skewed. A more important change is that a secondary oscillation appears in the loading for $11.65s < t < 11.8s$ in the cases D, E, F, G, and for $11.6s < t < 11.75s$ in case H. This secondary oscillation appears very abrupt in the cases F, G, H, exciting even small resonant pitching oscillations of the cylinder at 18.5 Hz. The duration of the secondary oscillation is in all examples approximately $0.15s$, which means about 15% of the wave period. The peak of the secondary oscillation occurs at $t \simeq 11.75s$ in the cases D, E, F, at $t \simeq 11.72s$ in case G and at $t \simeq 11.67s$ in case H. This means approximately one quarter period after the maximum of the loading occurring at $t \simeq 11.5s - 11.6s$.

There is no skewness in the incoming wave field which can explain the appearance of secondary oscillation in the recorded forces. It must be caused by a process in the fluid taking place in the near vicinity of the cylinder.

We note that the period of the secondary oscillations in the forces is much longer than the resonance period of the cylinder/beam. This justifies that the resonant oscillations in the force curves may be filtered out, as discussed in section 2. The resulting smooth force curves are shown for cases E - H in the figures 5a-d.

Smooting of the resonant oscillations in the force curves is unwanted, strictly speaking. We note, however, that the secondary oscillation in the force curves clearly is present in two cases which are not disturbed by resonant oscillations at $18.5Hz$. These cases are D and E, see figures 4d-e and figure 5a. The filtered force curves for the cases F - H show secondary oscillations being similar to the unfiltered secondary oscillations in case E.

It is of interest to estimate the height of the secondary oscillation occurring in the force measurements. Let δ_u and δ_l denote the height of the oscillation recorded at the upper and lower force transducers, respectively. δ_u and δ_l may then be estimated from figures 4b-d and 5a-d, as indicated in figure 5a. The values are shown in table 2. We have also listed in the table the total peak-to-peak values of the recorded forces during the time

6

case	δ_u	δ_l	Δ_u	Δ_l	δ_u/Δ_u	δ_l/Δ_l	$(\delta_u + \delta_l)/(\Delta_u + \Delta_l)$
B	0	0	4.7N	9.9N	0	0	0
C	0	0	6.3N	12.4N	0	0	0
D	0.2N	0.3N	7.2N	13.5N	3%	2%	2%
E	1.0N	1.0N	8.2N	15.3N	12%	7%	9%
F	1.3N	1.4N	9.5N	16.1N	14%	9%	11%
G	1.6N	1.6N	11.1N	16.8N	14%	10%	11%
H	1.3N	1.3N	11.4N	17.7N	12%	7%	9%

Table 2: Peak-to-peak values of the forces on the cylinder. δ_u: the height of the secondary oscillation at the upper force transducer, δ_l: the height of the secondary oscillation at the lower force transducer, Δ_u: the peak-to-peak value of the force at the upper transducer, Δ_l: the peak-to-peak value of the force at the lower transducer.

interval $11.2s < t < 12.2s$, for comparison. While δ_u and δ_l are zero in the cases B, C, and very small in case D, their values become appreciable in the cases E, F, G, H. We note that δ_u may be up to 14% of the recorded peak-to-peak value of the force history at the upper transducer. The sum of δ_u and δ_l is up to 11% of the peak-to-peak value of the total wave force.

δ_u and δ_l are in all examples found to be of almost equal value. This means that the secondary force oscillations recorded at the upper and lower transducers, located at $Z_u = 27.5cm$ above and $Z_l = 36cm$ below the mean water line, respectively, is equivalent to one secondary force oscillation with height $\delta_u + \delta_l$, acting at position $Z = 4.3cm$ below the mean water line. $Z = 4.3cm$ is of the order one cylinder radius.

We note that the values of δ_u and δ_l grow proportial to the value of the wave crest squared in the cases E, F and G. The maximal values of δ_u and δ_l occur in case G. There values then decrease for a still increasing incoming wave height.

4 Measurements of the surface elevation

4.1 The surface elevation along the centerline of the wave tank

In order to get more insight into the generation mechanism of the secondary oscillation revealed in the force measurements, the surface elevation of the fluid is recorded in vicinity of the cylinder with results shown in figures 6-7. In addition photos of the elevation at the cylinder's lee side are exhibited in figures 8. Two cases are considered when the secondary oscillation is present in the force measurements (E and G) and one case (C) when this oscillation is absent. The recordings of the surface elevation and the forces are simultaneous.

Let us introduce coordinates x, y, z, with the plane $y = 0$ coinciding with the wave tank's center plane and the plane $z = 0$ coinciding with the mean water level. The positive

x-axis is oriented towards the beach, with $x = 0$ corresponds to the position at the cylinder's front. The positive z-axis is upwards. First the surface elevation is considered as a function of the coordinate x along the centerline of the wave tank at time instants increasing from $11.5s$ to $12.0s$, see figures 6a-c. The figures illustrate how the incoming wave results in a considerable run up height at the cylinder's weather side occurring at $t \simeq 11.5 - 11.6s$. The elevation there then decreases gradually until a minimum elevation is reached at $t \simeq 11.8 - 11.9s$. The elevation at the cylinder's rear increases gradually up to a maximum value which equals the crest height of the incoming wave, practically speaking. This maximum occurs in all examples at $t \simeq 11.7s$. The elevation there then decreases gradually until a minimum elevation occurs at $t \simeq 12.0s$.

The examples shown indicate that the surface elevation along the center line of the wave tank is smooth. There is one exception, however, in case G. A scatter in the recordings close to the cylinder's rear at $t = 11.7s$ is revealed in figure 6c. This scatter is due to a spray in the experiments. The surface elevation along the tank's center line is smooth, however, for locations being in-between $\sim 5cm$ and $\sim 20cm$ behind the cylinder's rear, where the latter value corresponds to the location where the spilling event starts.

We note that no secondary oscillations occur in the elevations at the cylinder's front and rear which can explain the secondary oscillation occurring in the force measurements for $11.6s < t < 11.8s$.

4.2 The surface-profile across the wave tank

The surface elevation is then considered as a function of the coordinate y across the wave tank at a location $5cm$ behind the cylinder's rear, for time instants increasing from $t = 11.5s$ to $t = 12.0s$. $5cm$ means 84% of the cylinder radius. The results are displayed in figures 7a-c, revealing that a complex flow dynamics is taking place at the cylinder's lee side for $11.6s < t < 12.0s$. Before discussing the details in figures 7 we note that the elevation close to the tank walls is, practically speaking, not affected by the presence of the cylinder for $t < 12s$.

Consider then the elevation at each time instant. For $t = 11.5s$ the elevation is almost constant across the tank. For $t = 11.6s$ the elevation is lower at the center of the tank than at the tank walls, which may be explained by a phase delay of the crest in the middle of the tank due to the presence of the cylinder. At $t = 11.7s$ in the cases C and E, and at $t = 11.65$ in case G, the wave crest has arrived at the recording position. The elevation is then the same at the tank walls ($y = \pm20cm$) and at the tank's center line ($y = 0cm$). A depression occurs in the elevation in-between $y = 0cm$ and $y = \pm20cm$, however. This depression is small in case C, but occurs with increasing strength in the cases E and G. By comparing figures 7a-c we remark that the difference in the elevation at the tank wall and the trough grows proportional to the value of ζ_{max} squared, roughly speaking.

In case G the elevation formes a cusp at $y = 0$ for $t = 11.65s$. This cusp remains for $11.65s < t < 11.8s$. The depression in ζ, occurring for $2cm < |y| < 15cm$, lasts during the same time interval. For $t > 11.8s$ the depression has disappeared. The cusp then develops into a smooth elevation which disintegrates into two crests propagating towards the tank walls ($t = 11.85s - 12s$). In case E a pronounced depression occurs in ζ for

$3 - 4cm < |y| < 20cm$ during the time interval $11.7s < t < 11.8s$. During the same time interval there is an elevation at the center of the wave tank, for $|y| < 3 - 4cm$, exceeding the value of ζ at the tank walls. This elevation disintegrates into two crests propagating towards the tank walls for $t > 11.9s$, as in case G. In case C the dynamics of ζ is similar to that in E and G, but is far more weak, however.

The flow dynamics leading to the surface profiles revealed in the figures 7a-c is certainly complex. It is, however, not the intention to explain all the details of this process in the present contribution. On the other hand, we note that the depression in the surface elevation is present during the time interval $\sim 11.65s < t < \sim 11.8s$. We also note that the elevation increases at the center of the wave tank when the wave crest has left the recording position. This occurs when the fluid acceleration is negative at the cylinder position. This increase of the surface elevation is a counterpart of the run-up at the front of the cylinder.

5   Discussion

In the cases C and E we note that the depression in the surface elevation behind the cylinder occurs for $11.7s < t < 11.8s$. In case G the corresponding depression occurs for $11.65s < t < 11.8s$. The horizontal particle velocity of the fluid, U_0, is positive at the cylinder position during these time intervals. U_0 becomes zero at the cylinder position, however, for $t \simeq 11.8s$. We remark that the depression in the surface elevation occurs during the same time interval as the secondary oscillations occur in the force recordings.

The major trend in the force curves during the time interval $11.5s < t < 11.8s$ are decreasing forces. This is firstly due to that the local horizontal fluid acceleration is negative, and secondly due to that the difference between the elevations at the front and rear of the cylinder is decreasing monotonously, giving a monotonous decay in the hydrostatic force on the cylinder. The secondary force oscillation is, however, always a positive force. These facts indicate that a low-pressure is present in the fluid behind the cylinder for $11.65s < t < 11.8s$, and that the secondary force oscillation is a suction force.

The suction force appears in the measurements when the wave crest is about one cylinder radius behind the cylinder's rear and reaches a maximum when the wave crest is about one cylinder diameter behind the cylinder's rear. Under the wave crest the horizontal fluid acceleration vanishes. The horizontal particle velocity has, on the other hand, a maximal value there. Let this maximal value be denoted by U_m. The experimental results thus indicate that the magnitude of U_m plays an important role in the problem.

The force measurements have revealed that the secondary force oscillation may be represented by a horizontal force vector acting at a vertical position of the order one cylinder radius below the free surface. This indicates that the suction force is due to a free surface effect, i.e. the effect due to the acceleration of gravity. The cylinder diameter is obviously the appropriate length scale for the local flow around the cylinder. A non-dimensional particle velocity is then given by the local Froude number, i.e.

$$Fr = U_m/(gd)^{1/2} \qquad (1)$$

where $g = 9.81ms^{-2}$ denotes the acceleration due to gravity. The value of U_m may be

case	$\zeta_{max}\omega/(gd)^{1/2}$
A	0.08
B	0.20
C	0.29
D	0.35
E	0.41
F	0.47
G	0.52

Table 3: The Froude number due to the maximal particle velocity at the cylinder position based on the cylinder diameter.

estimated by

$$U_m \simeq \zeta_{max}\omega \tag{2}$$

where ζ_{max} is the local crest height and $\omega = 2\pi/P$, where P denotes the local wave period, being in all our examples $P \simeq 1s$. We note that (2) is not an appropriate measure of the particle velocity under the wave crest in case H, since the wave in this case develops to a plunging breaker. The Froude number given by (1) and (2) are then obtained in table 3 for the cases A-G. For illustration we also show in figure 9 the nondimensional peak-to-peak values of the secondary oscillations in the force, $\delta_u + \delta_l$, based on the values obtained in table 2, as a function of the Froude number. In the cases A-C the Froude number is less than 0.3. Then the secondary oscillation is absent in the experiments. In case D the Froude number is 0.35. Then the secondary force oscillation appears in the experiments. In the cases E - G the Froude number exceeds 0.4. Then the secondary force oscillations are pronounced. The latter results may be interpreted in the following way. The fluid flow around the cylinder is effectively a horizontal current during the small part of the wave period when the wave crest is passing the cylinder, with local velocity U_m at the crest. The forced wave due to this current has a wave length given by linear theory, being

$$\lambda_U = 2\pi U_m^2/g \tag{3}$$

We note that pronounced nonlinear effects may take place in the flow close to the cylinder. Nonlinear wave theory give, however, only minor changes in the value of λ_U given by (3). For $Fr \simeq 0.4$ we have that $\lambda_U \simeq d$. A resonance between the free surface and the body may then take place. For $Fr > 0.4$ we have that $\lambda_U > d$. A resonance between the free surface and the body is still possible, however. Our results thus indicate that the Froude number is an important parameter in the problem.

A parallell to the secondary force oscillation appearing in the experiments may be the wave resistance experienced by ships with great draught. The wave resistance is equivalent to a suction force acting at the ship's rear. It is well known that dispacement ships become good wave makers, introducing a considerable wave resistance, when the Froude number based on the ship length exceeds the value of 0.35 − 0.4, see e.g. Newman (1977, pp. 281-284).

case	λ	ζ_{max}	H
C	349m	11.0m	16.7m
D	353m	13.5m	19.6m
E	355m	15.8m	22.5m
F	365m	18.0m	26.3m
G	369m	20.0m	29.0m

Table 4: Wave characteristics in large scale, cases C − G. The local wave period is $15s$.

It is of interest to relate the time and length scales in the model to large scales. If the local wave period in large scale is $15s$, i.e. a ratio between the time in the model scale and the large scale being $1 : 15$, the ratio between the length in the model scale and the large scale is $1 : 225$. This means that in large scale the cylinder diameter is $d = 26.8m$. The corresponding values of λ, ζ_{max} and H in large scale are shown in table 4 for the cases C − G.

6   Conclusion

An experimental study of the wave loads on a restrained vertical circular cylinder is presented. The wave height is varied between a small value, being in the regime of linear wave theory, up to a great value leading to a plunging breaker. The wave loads are proportional to the fluid acceleration for small and moderate wave height. When the wave height exceeds a certain value, however, a secondary oscillation occurs in the wave loading. The secondary oscillation occurs about one quarter wave period after the main peak in the loading. It starts when the wave crest is about one cylinder radius behind the cylinder's rear and reaches a maximum when the wave crest is about one cylinder diameter behind the cylinder's rear. It then decays to zero. The secondary force oscillation lasts for about 15% of the wave period, has a magnitude up to 11% of the peak-to-peak value of the total force and has a resultant acting approximately one cylinder radius below the mean water line. The experiments indicate that the secondary force oscillation is a suction force. Moreover, we find that the Froude number based on the particle velocity at the wave crest, the cylinder diameter and the acceleration due to gravity, i.e. $Fr = U_m/(gd)^{1/2}$, is an important parameter in the problem. We find that the secondary oscillation appears in the force measurements when $Fr = 0.35$, and that the secondary oscillation is pronounced for $Fr > 0.4$.

11

References

[1] CHAU, F. P. AND EATOCK-TAYLOR, R. (1992) Second-order wave diffraction by a vertical cylinder. J. Fluid Mech. **240**, pp. 571-599.

[2] DOMMERMUTH, D. G., YUE, D. K. P., LIN, W. M., RAPP, R. J., CHAN, E. S. AND MELVILLE, W. K. (1988), Deep-water plunging breakers: a comparison between potential theory and experiments. J. Fluid Mech. **189**, pp. 423-442.

[3] EATOCK-TAYLOR, R. AND HUNG, S. M. (1987) Second-order diffraction forces on a vertical cylinder in regular waves. Appl. Ocean Res. **9**, pp. 19-30.

[4] GRUE, J. (1992) Nonlinear water waves at a submerged obstacle or bottom topography. J. Fluid Mech. **244**, pp. 455-476.

[5] KIM, M. H. AND YUE, D. K. P. (1989) The complete second-order diffraction waves around an axisymmetric body. J. Fluid Mech. **200**, pp. 235-262.

[6] NEWMAN, J. N. (1977) Marine hydrodynamics. The MIT press.

[7] ZHOU, D., CHAN, E. S. AND MELVILLE, W. K. (1991) Wave impact pressures on vertical cylinders. Appl. Ocean Res. **13**, pp. 220-234.

Figure captions

Figure 1.
Time history of the displacement of the wave generator, $X(t)$ (in cm), as a function of time t (seconds), for $\alpha = 1$.

Figure 2.
Sketch of the profile of the leading wave in the wave group at the location of the cylinder axis. The cylinder is absent. ζ_{max}: the local crest height, H: the local wave height, λ: the local wave length.

Figure 3.
Time histories of the recorded surface elevation ζ_0 at the location of the cylinder axis. a) case E for $9s < t < 14s$, b) case B for $11s < t < 12.4s$, c) case C for $11s < t < 12.4s$, d) case E for $11s < t < 12.4s$, e) case G for $11s < t < 12.4s$, f) case H for $11s < t < 12.4s$.

Figure 4.
Recorded forces in $Newton$ (N). Solid line: The upper force transducer. Dashed line: The lower force transducer. a) case E for $9s < t < 14s$, b) case B for $11s < t < 12.4s$, c) case C for $11s < t < 12.4s$, d) case D for $11s < t < 12.4s$, e) case E for $11s < t < 12.4s$, f) case F for $11s < t < 12.4s$, g) case G for $11s < t < 12.4s$, h) case H for $11s < t < 12.4s$.

Figure 5.
The secondary oscillation in the force histories. Solid line: The force history at the upper transducer, with the resonant oscillation at $18.5Hz$ filtered out. Dashed line: The force history at the lower transducer, with the resonant oscillation at $18.5Hz$ filtered out. Sparce dotted lines: The unfiltered force histories. a) Case E, $11.6s < t < 11.9s$, b) Case F, $11.6s < t < 11.9s$, c) Case G, $11.6s < t < 11.9s$, d) Case H, $11.55s < t < 11.85s$.

Figure 6.
Surface elevation as a function of the coordinate x (in cm) along the center line of the wave tank. $x = 0$ corresponds to the position at the cylinder's front. Different time instants: $t = 11.5s, 11.6s, 11.7s, 11.8s, 11.9s, 12.0s$.
a) Case C, b) Case E, c) Case G.

Figure 7.
Surface elevation as a function of the transverse coordinate y (in cm) at a location $5cm$ behind the cylinder's rear. Natural scale. Different time instants: $t = 11.5s, 11.6s, 11.65s, 11.7s, 11.75s, 11.8s, 11.9s, 12.0s$. a) Case C, b) Case E, c) Case G.

Figure 8.
Photographs of the surface elevation at the cylinder's rear. Case E. A wave gauge is seen at the center line of the wave tank $1cm$ behind the cylinder's rear. The black marks on the cylinder are at heights $5cm$ and $10cm$ above the mean water line. a) $t \simeq 11.67s$, b) $t \simeq 11.7s$, c) $t = 11.8s$.

Figure 9.
Non-dimensional peak-to-peak values of the secondary oscillation in the force, $\delta_u + \delta_l$, vs. local Froude number.
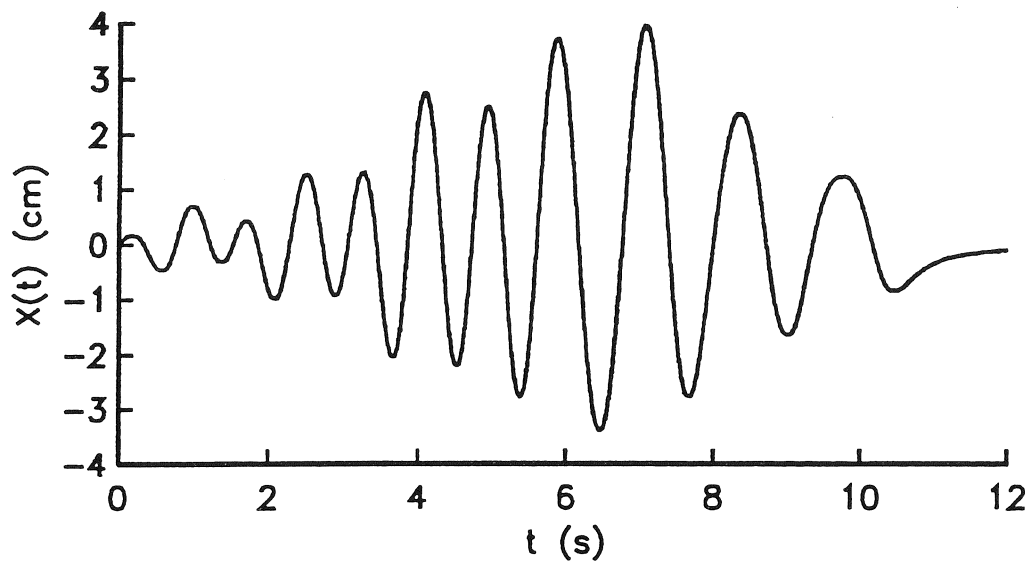
Figure 1.
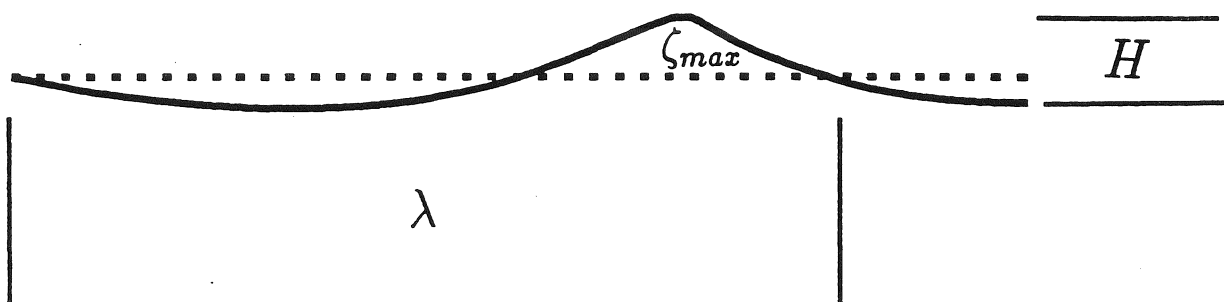
Figure 2.
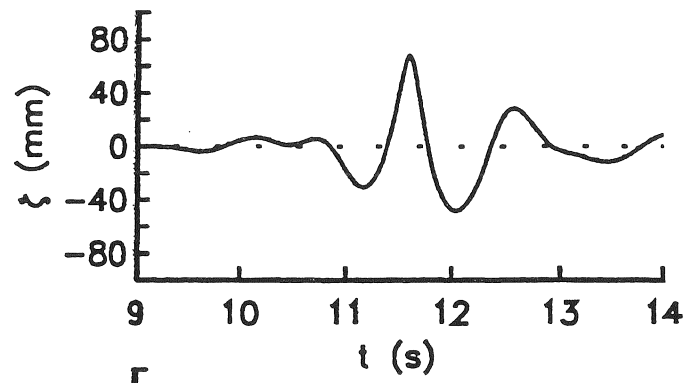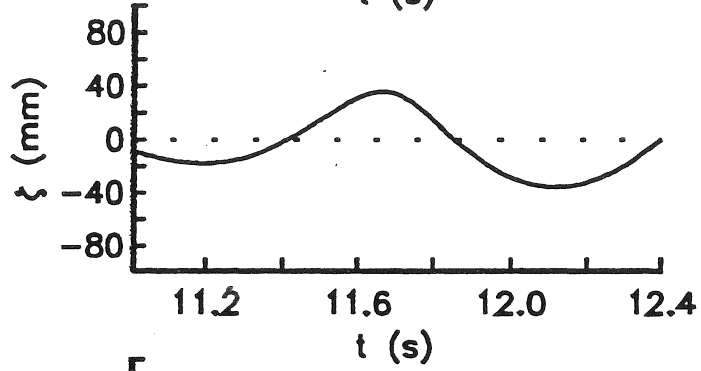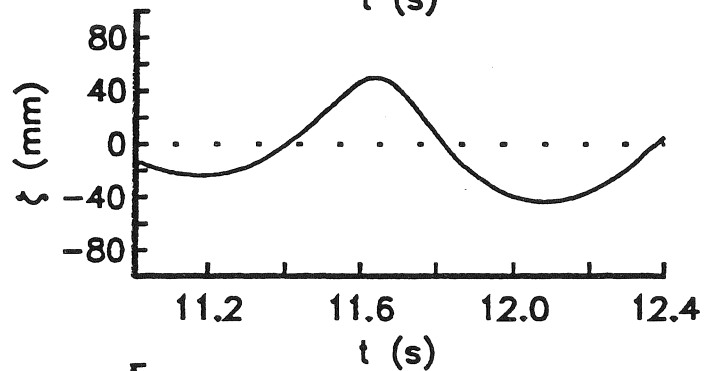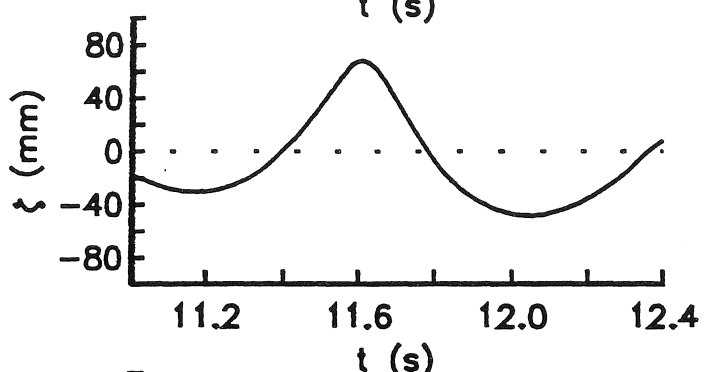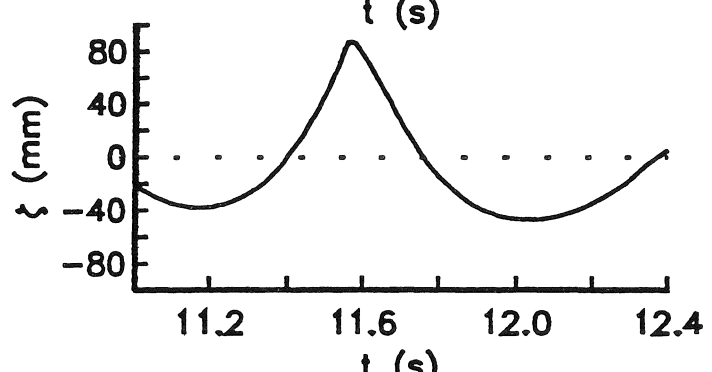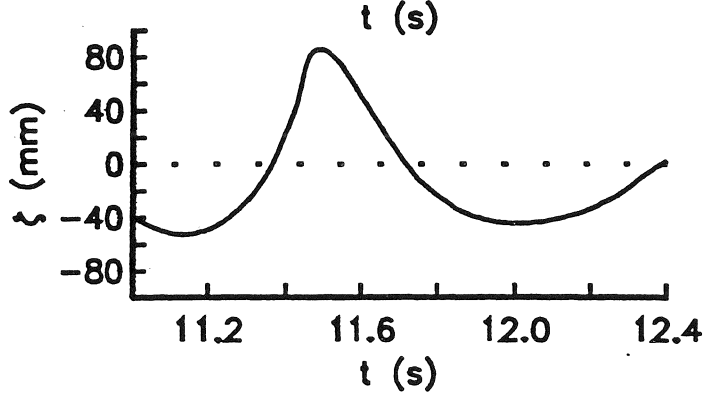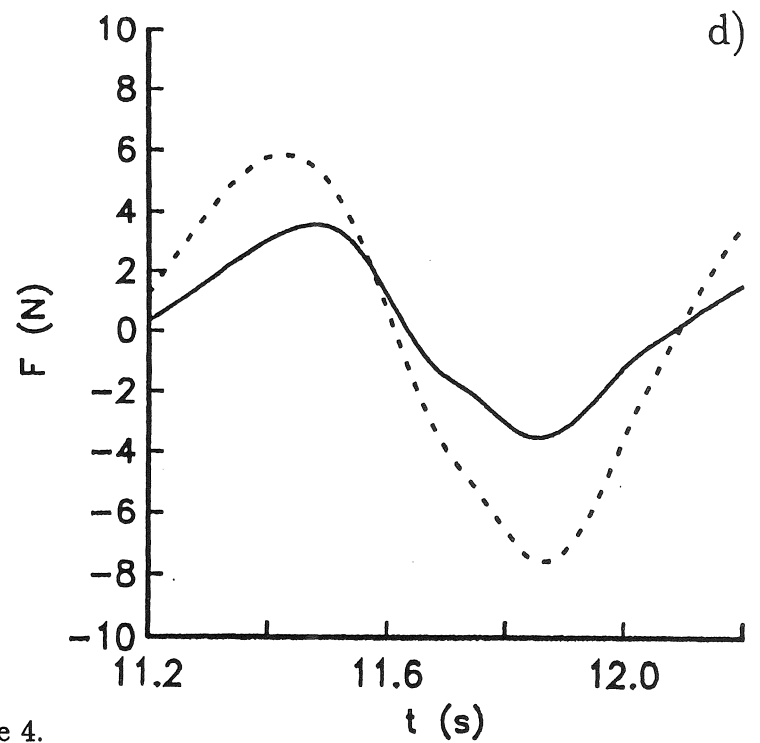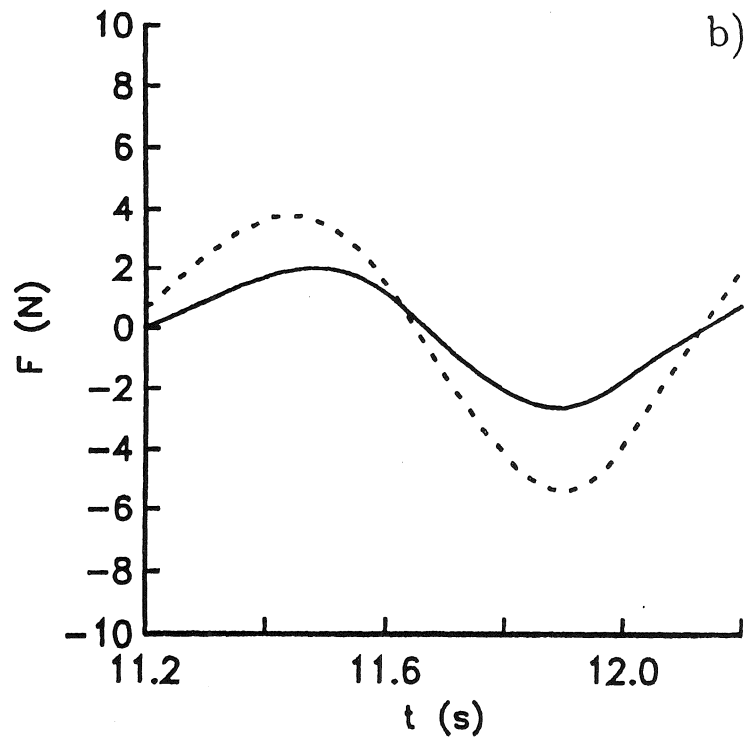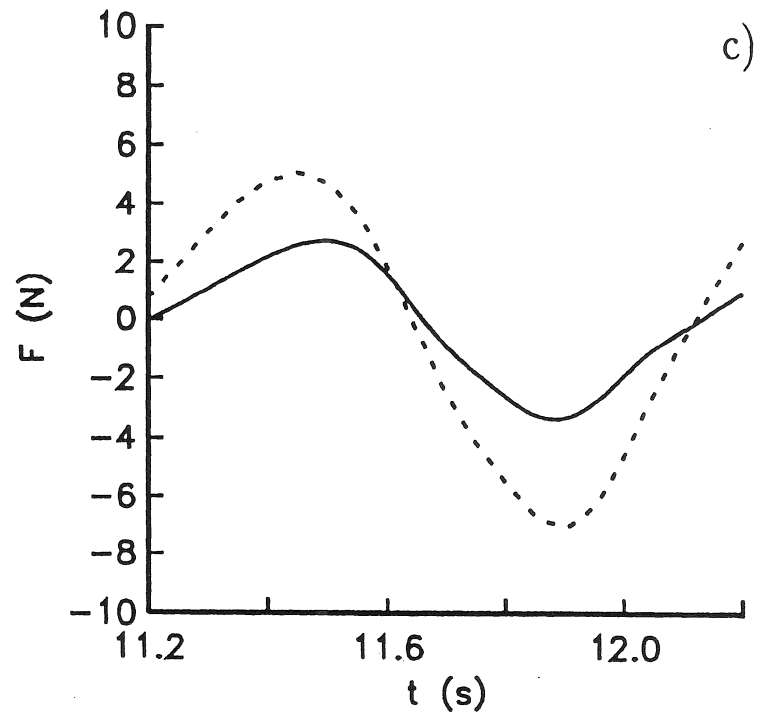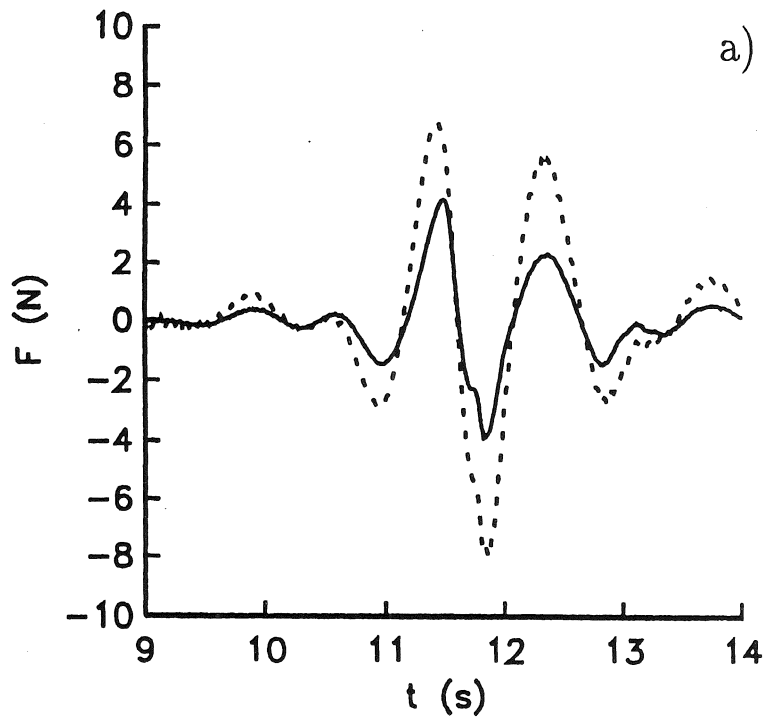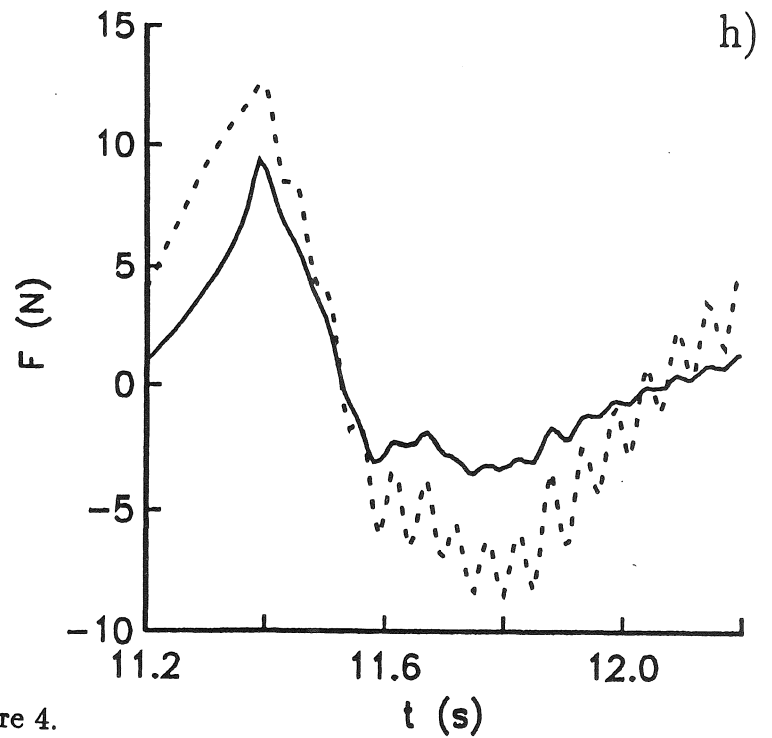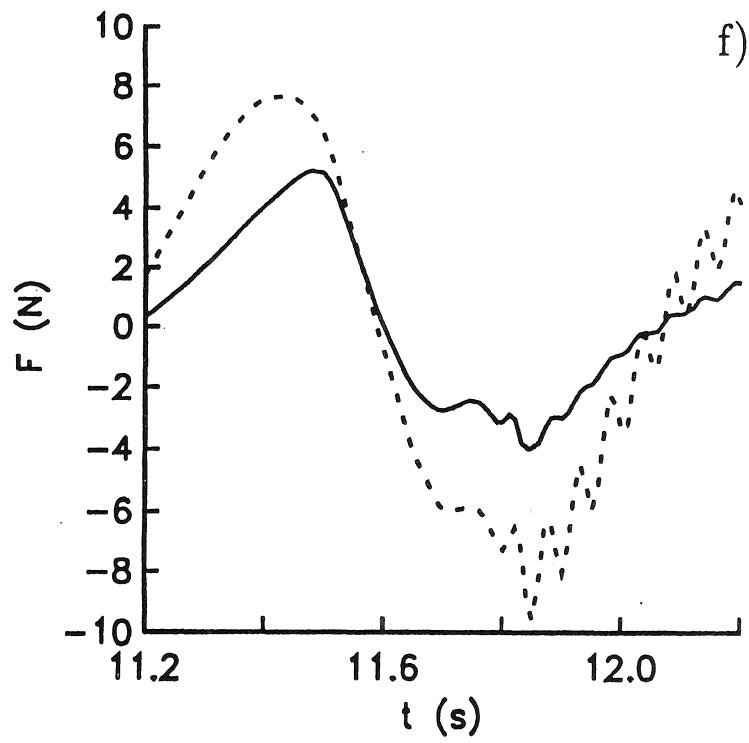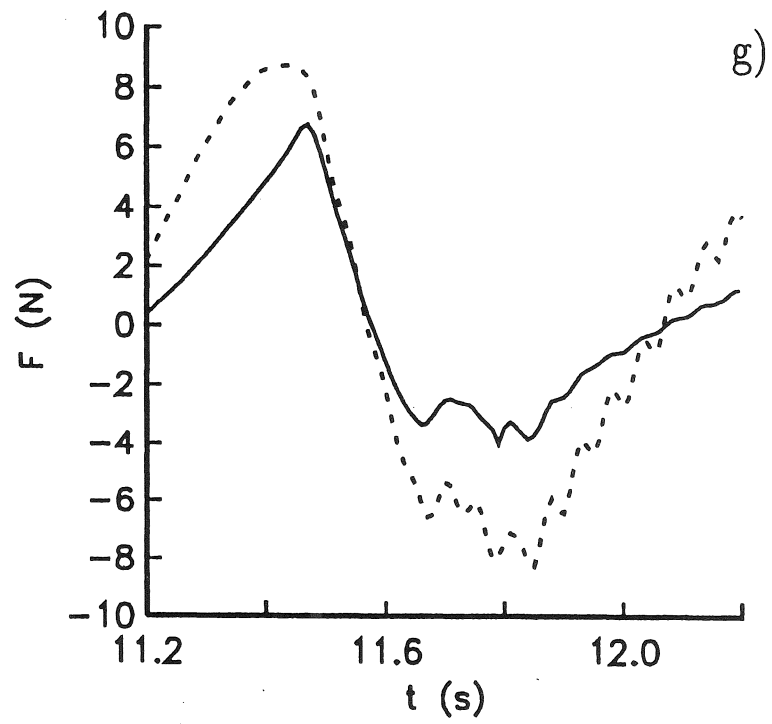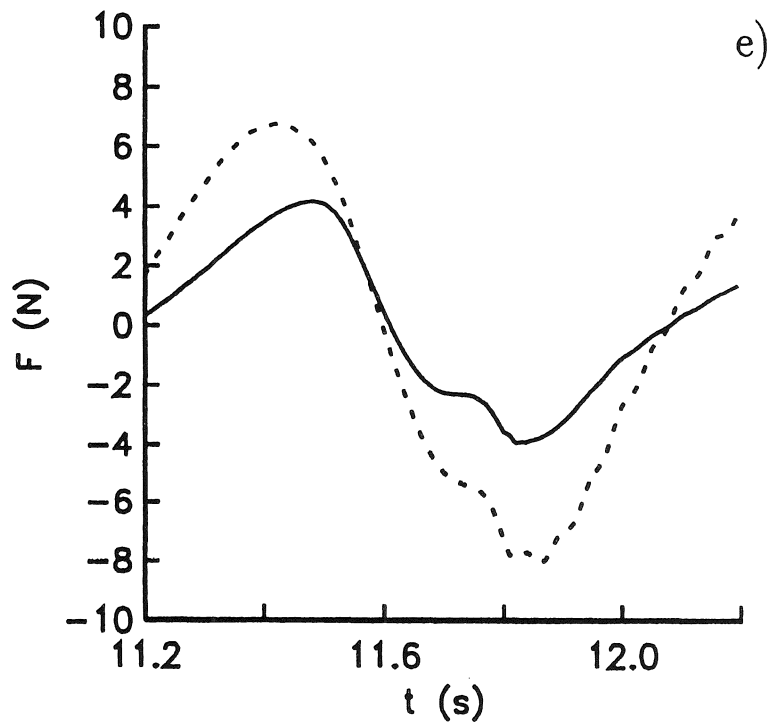
Figure 3.

Figure 4.
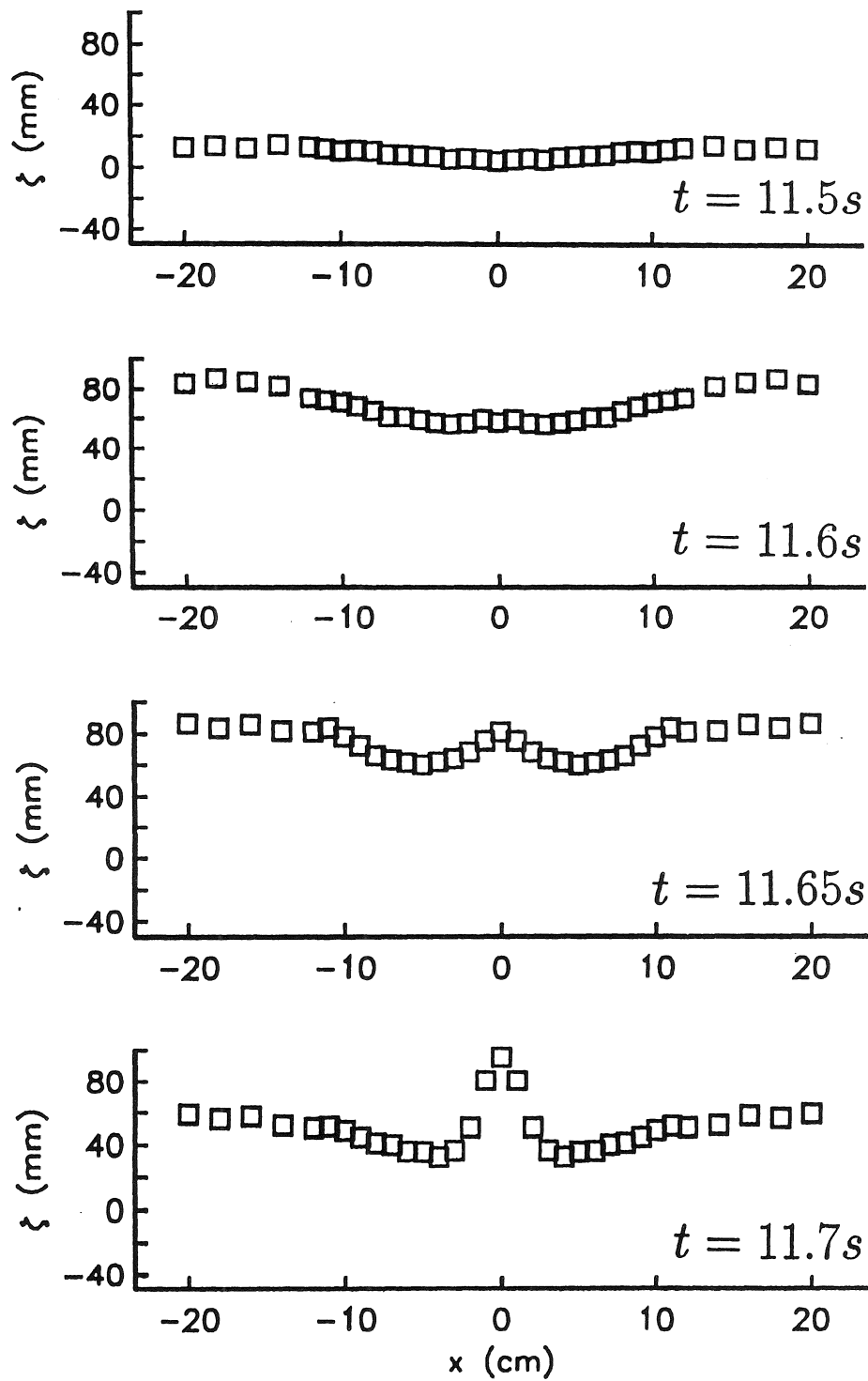
Figure 4.
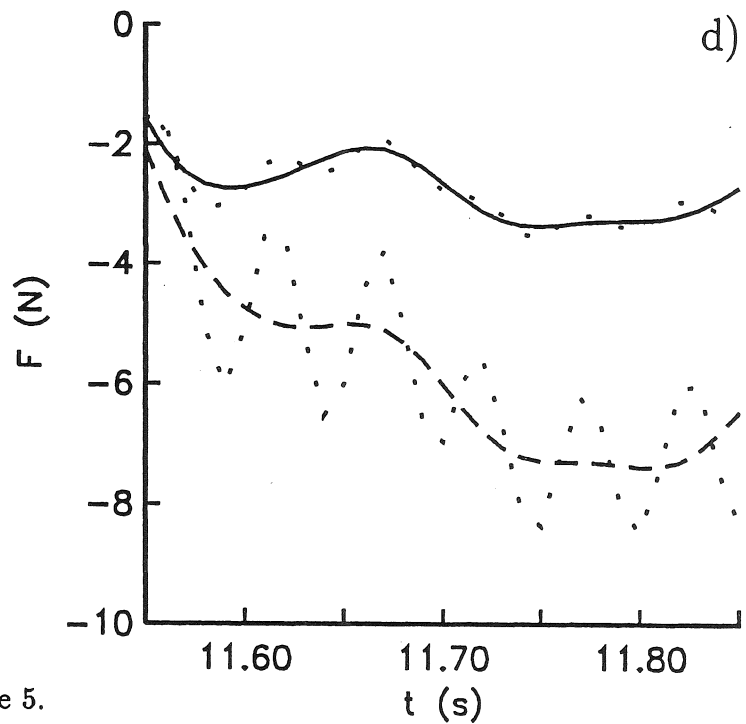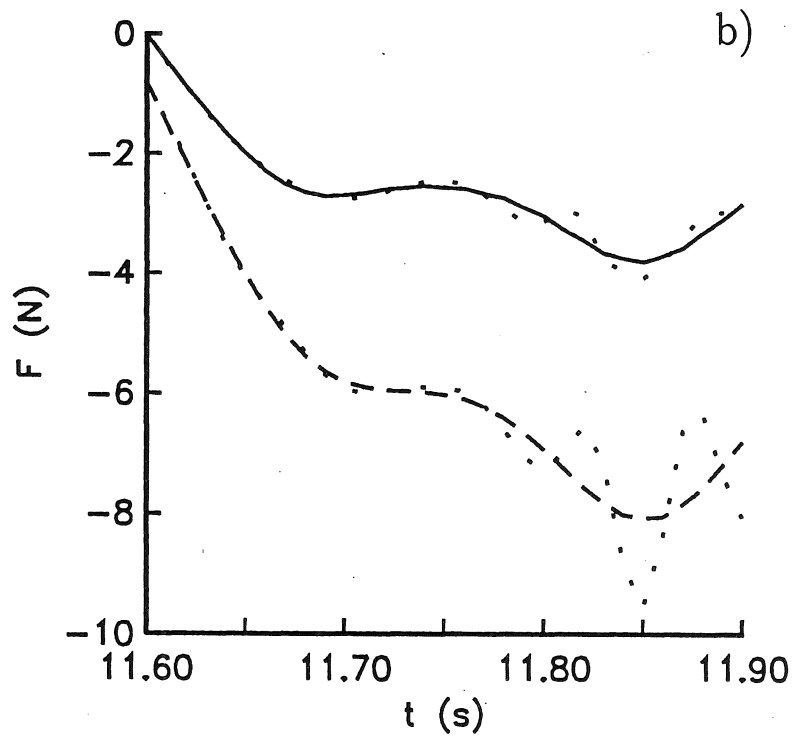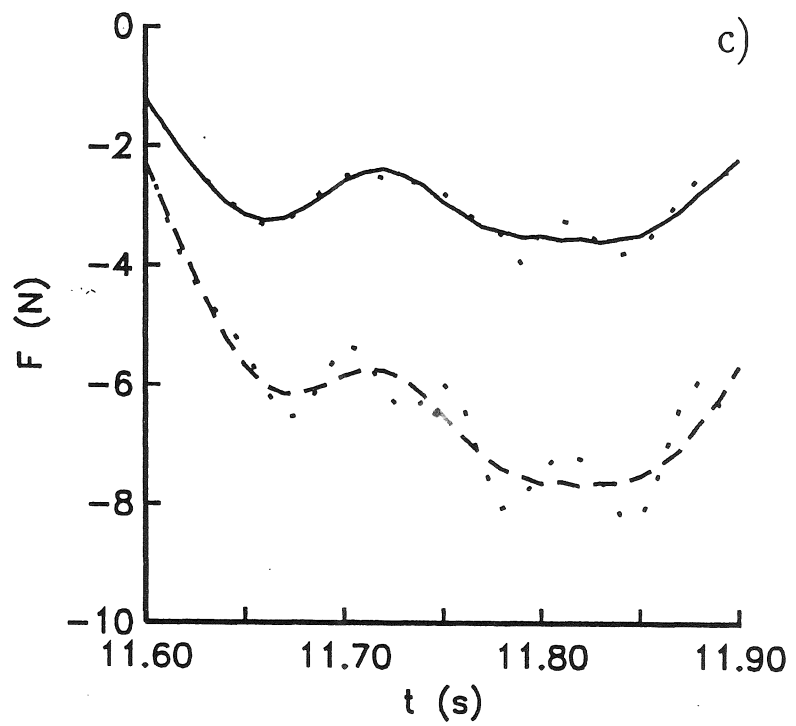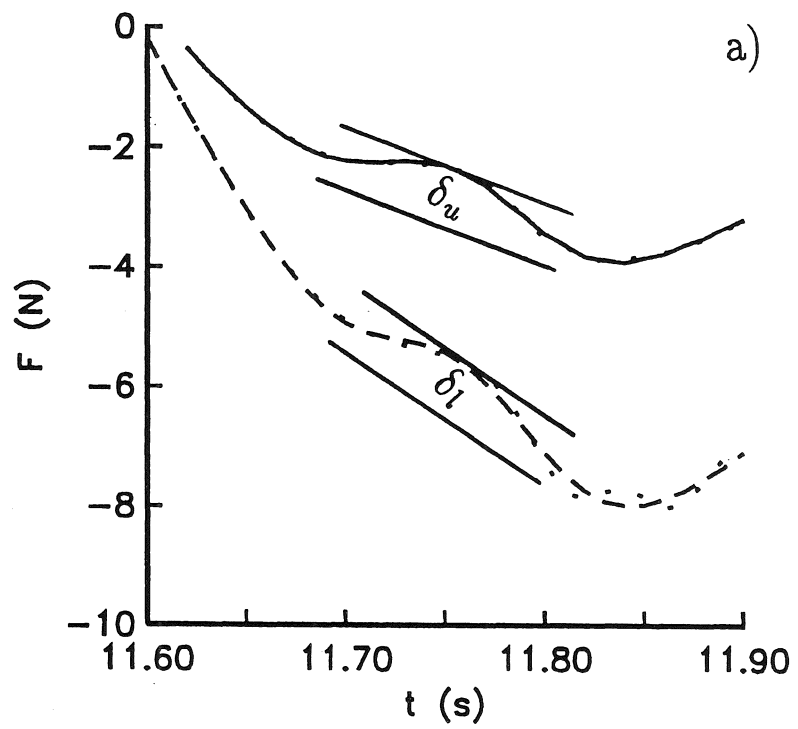
Figure 5.

a)
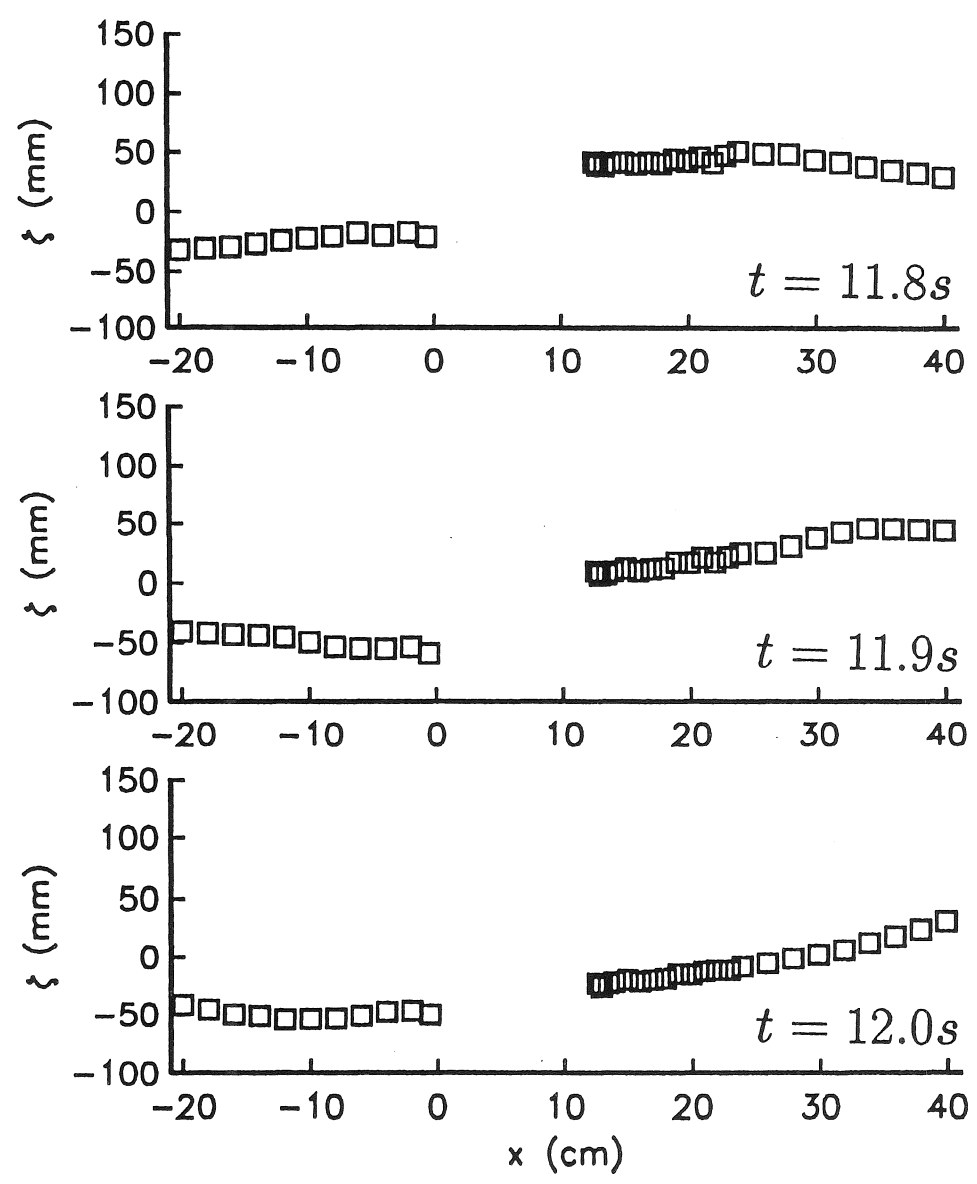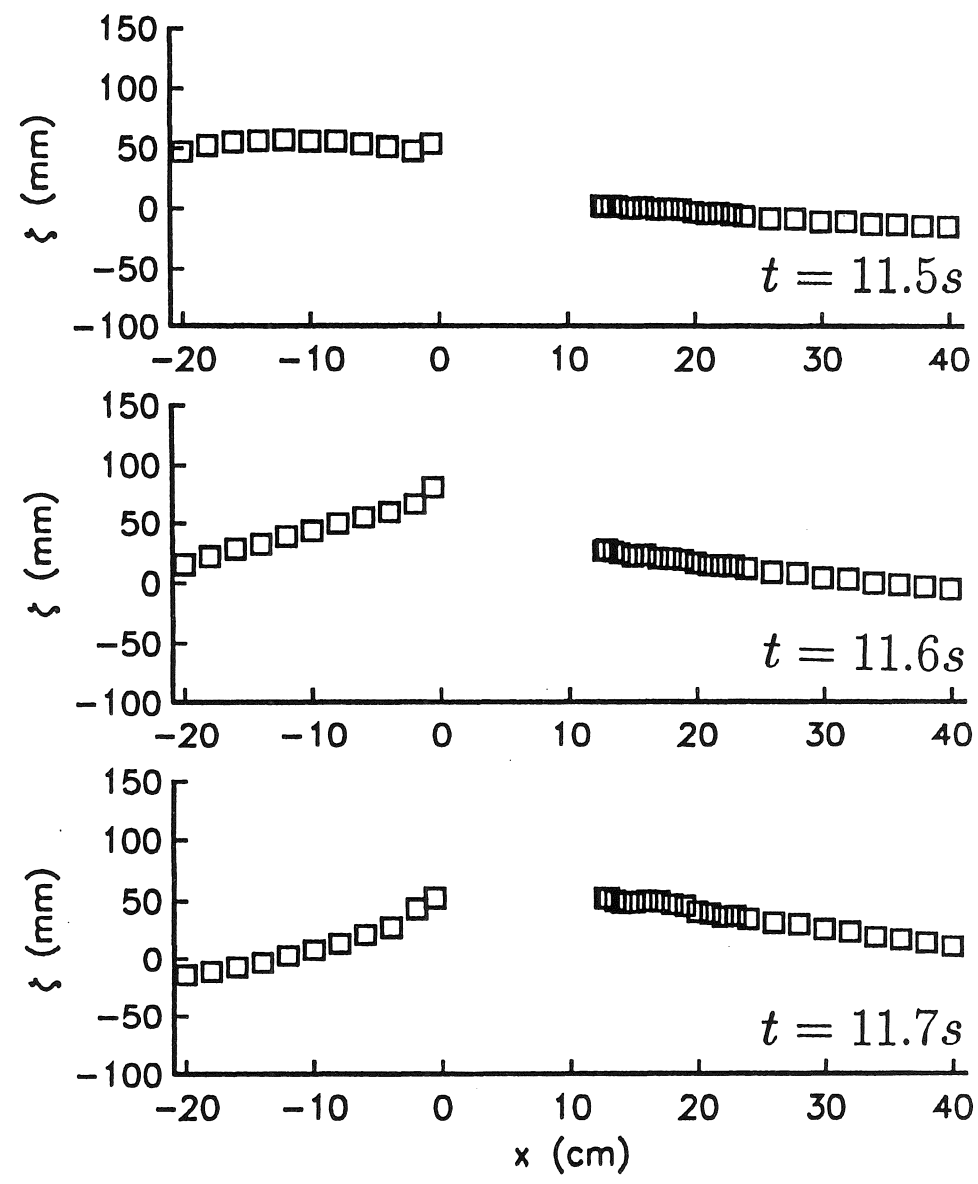
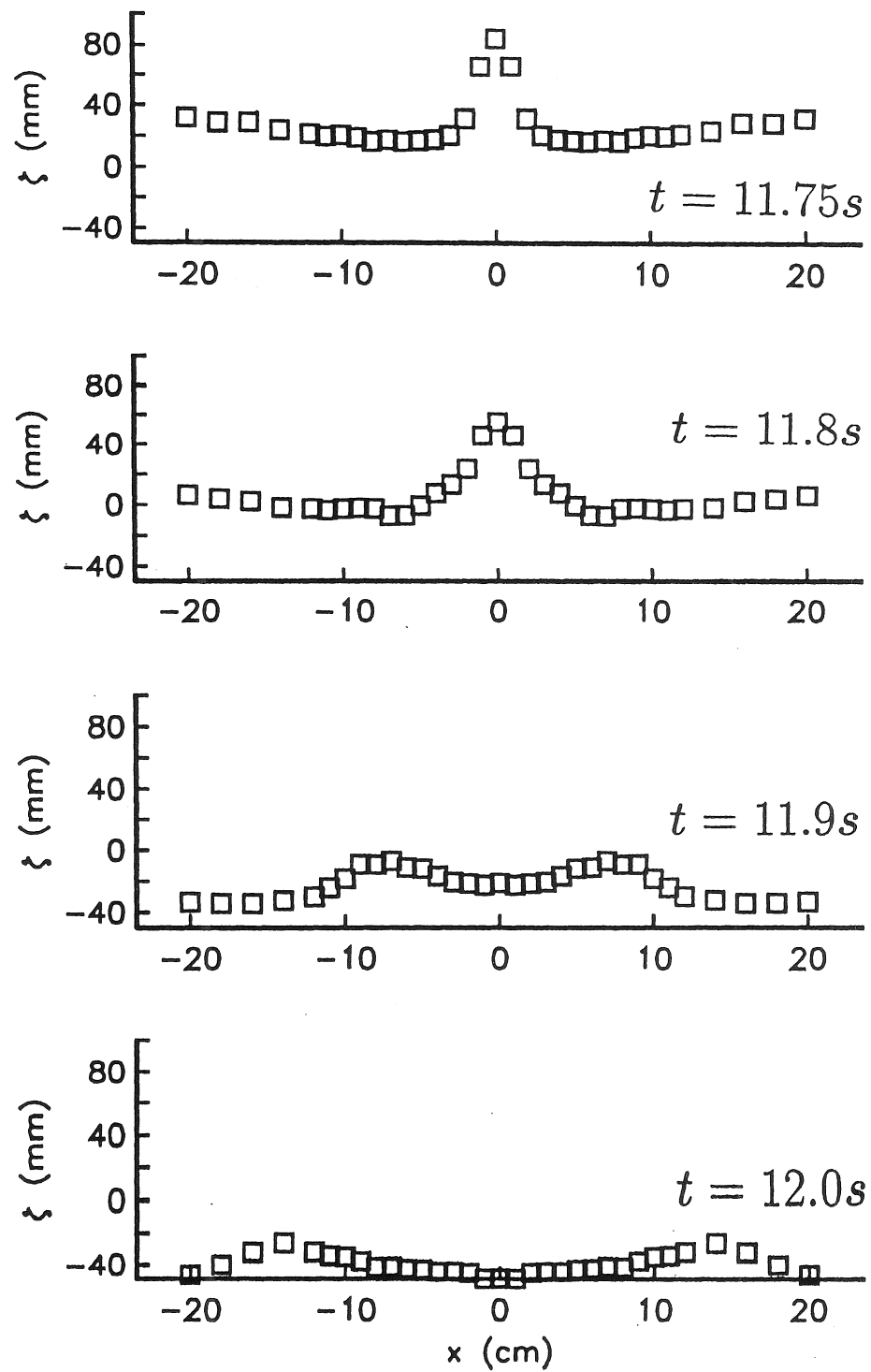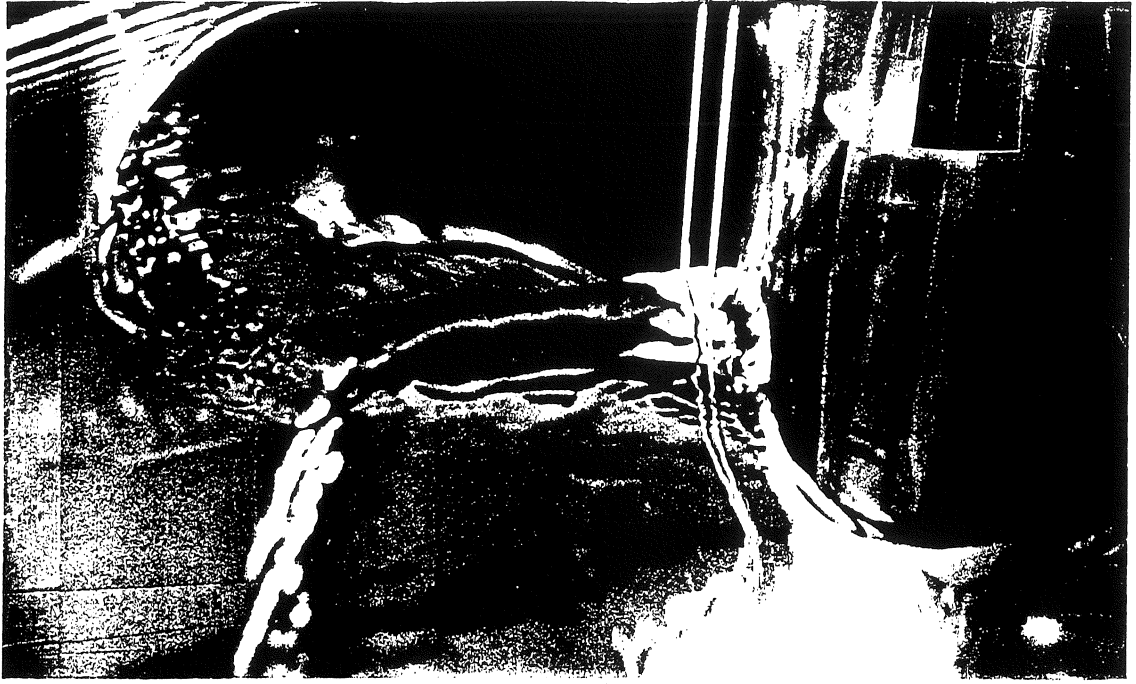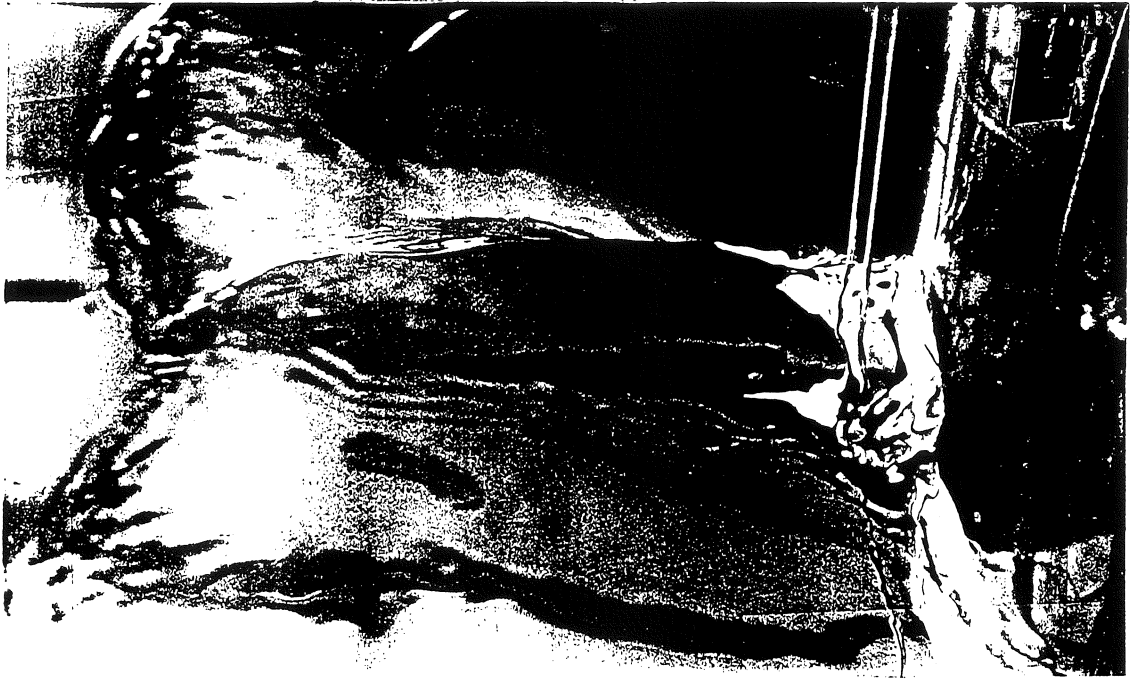Figure 6.

b)
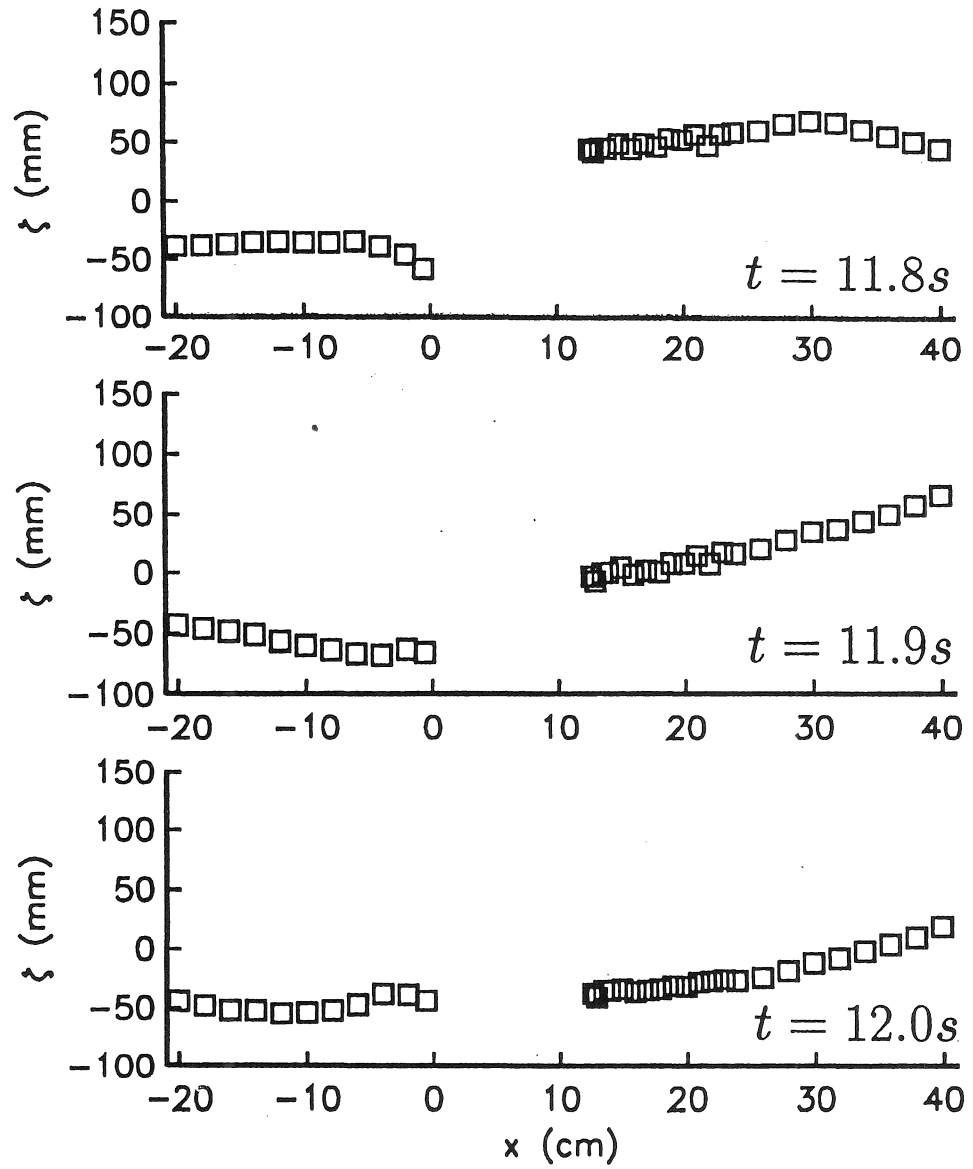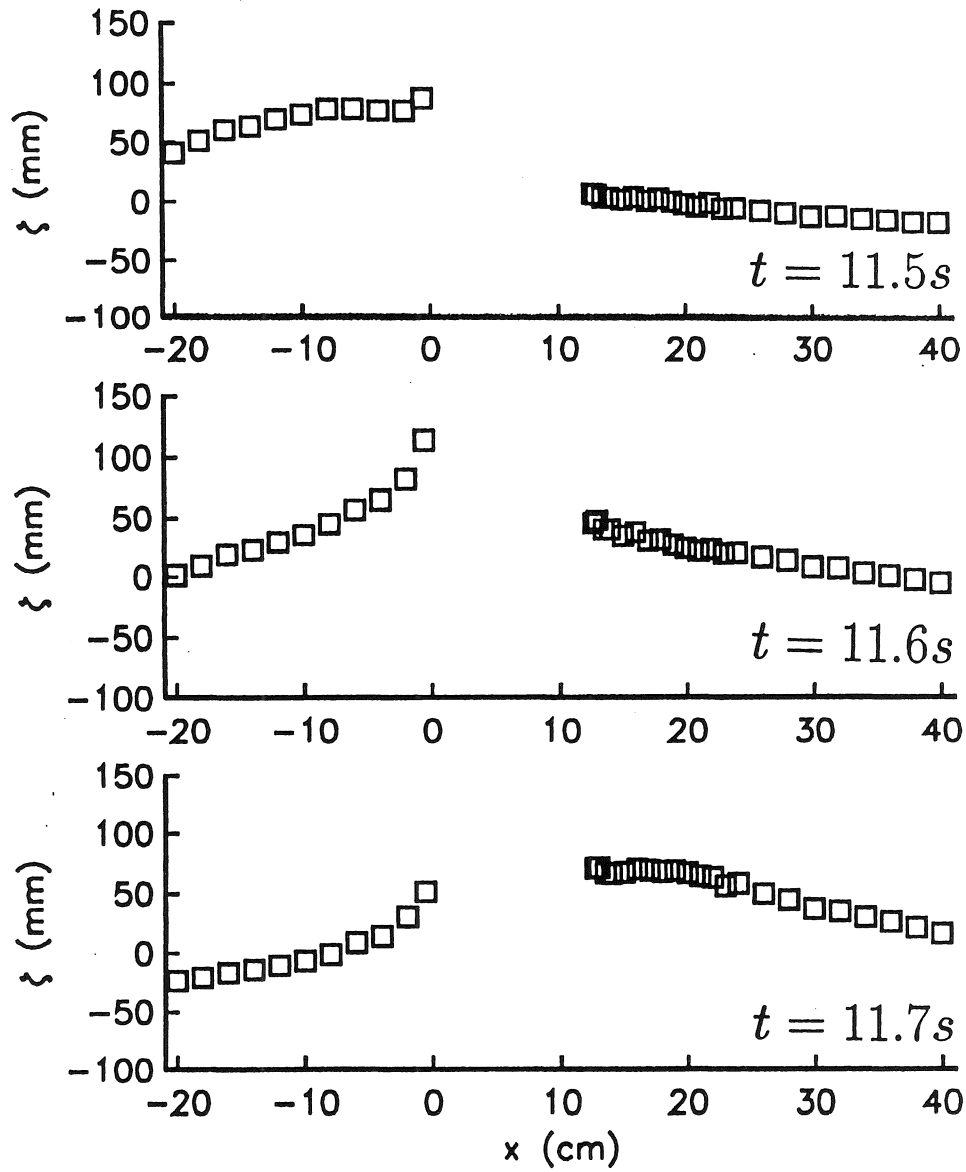
Figure 6.

c)
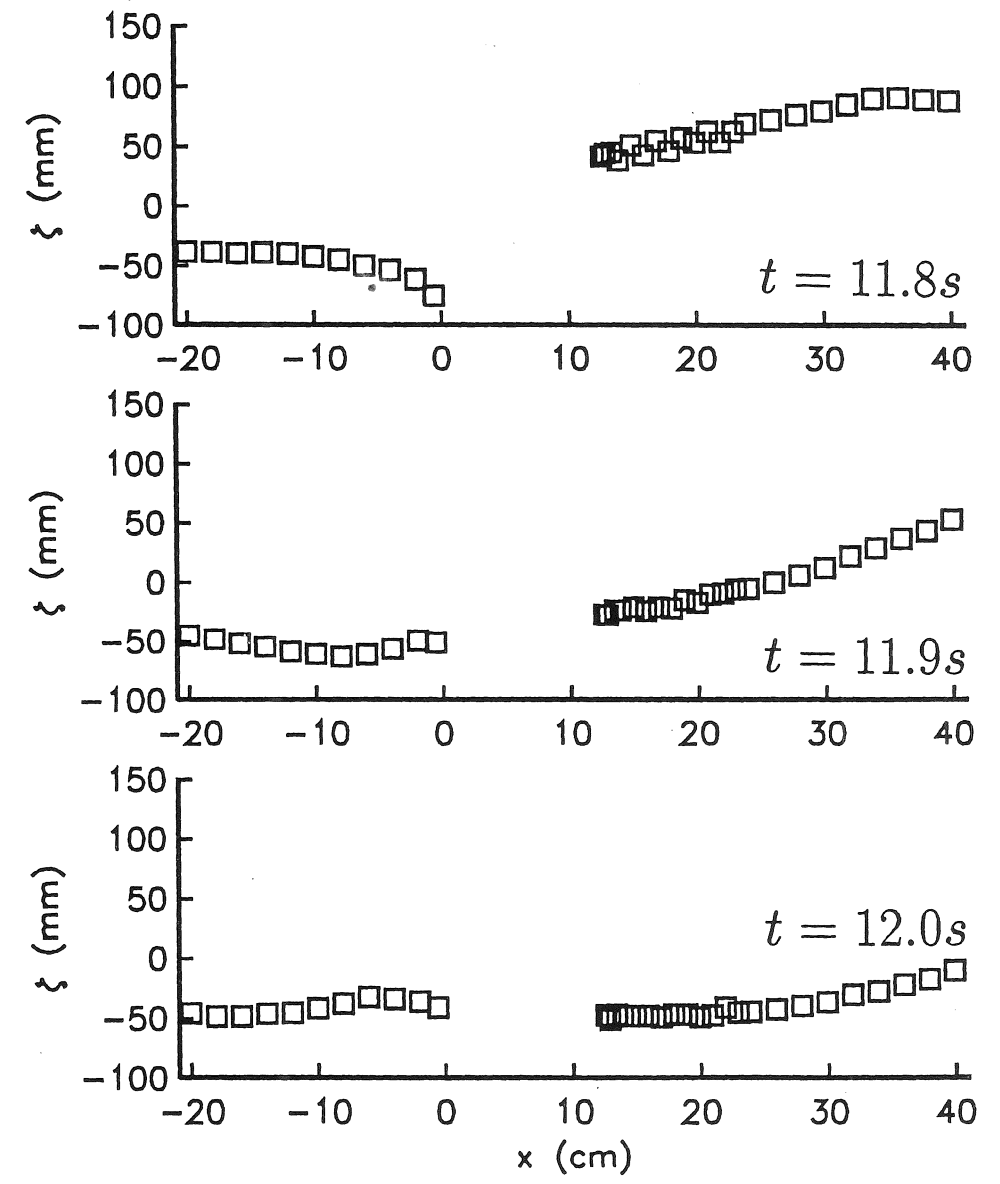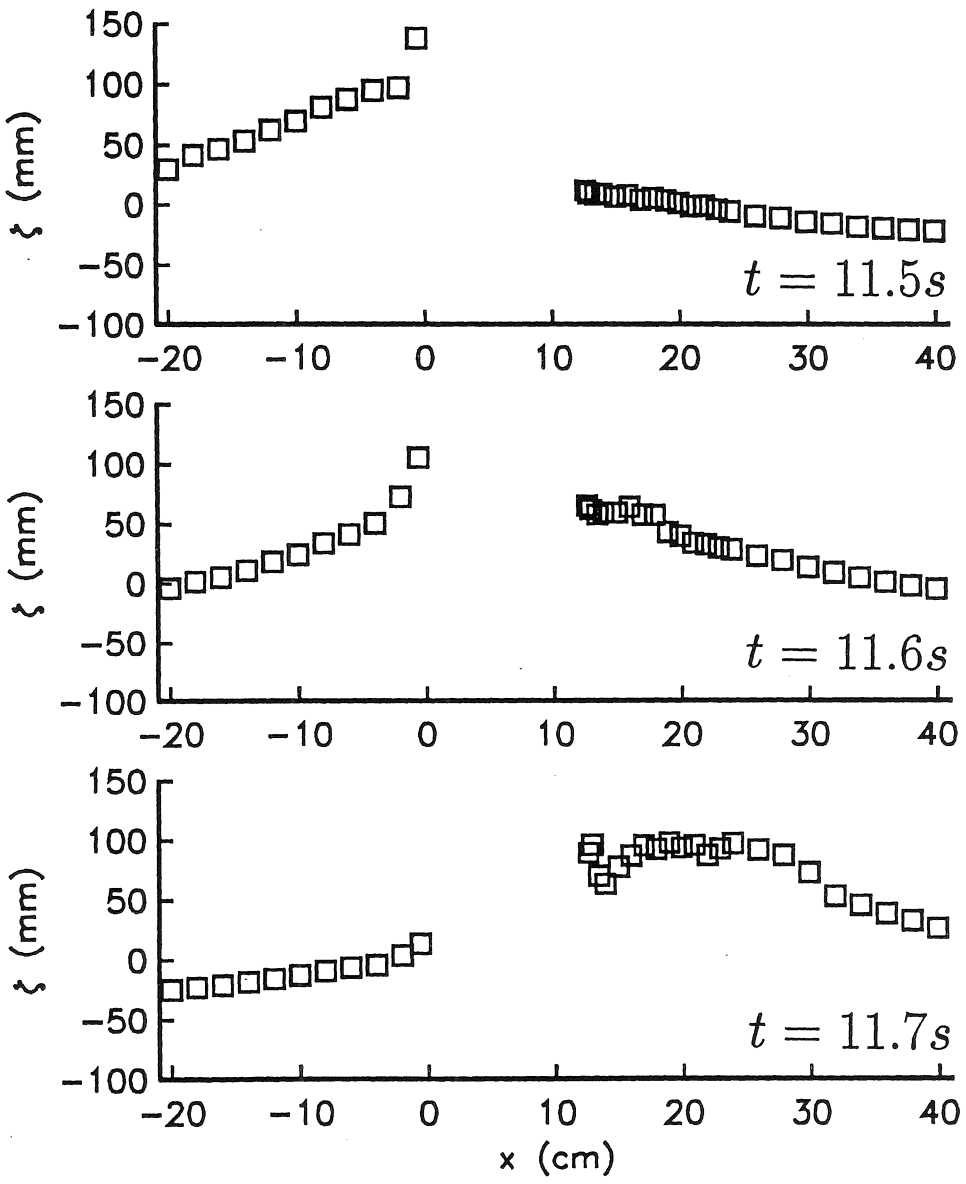
Figure 6.
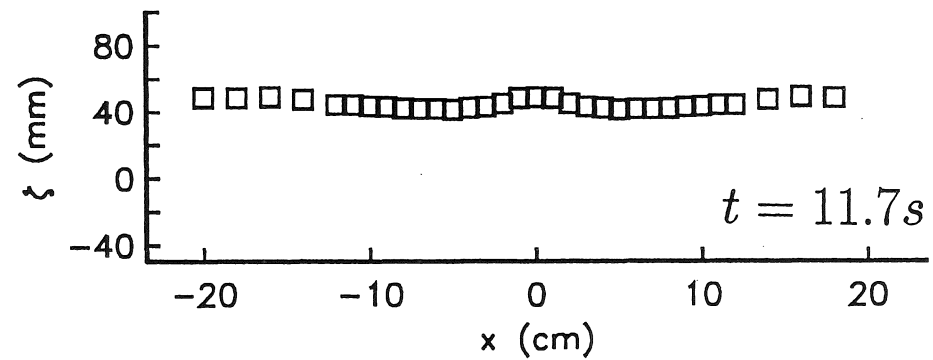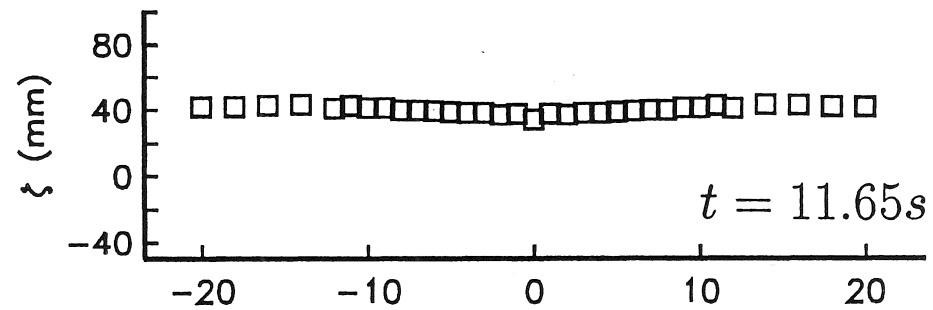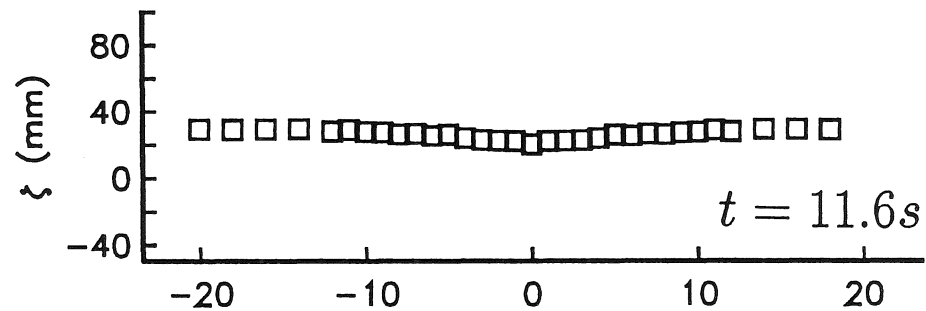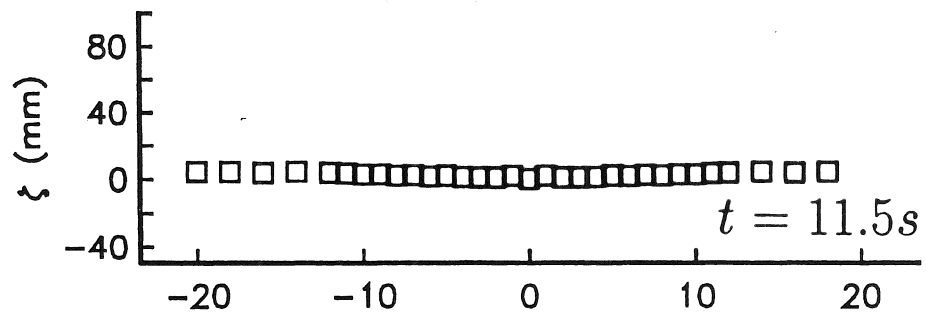
a)
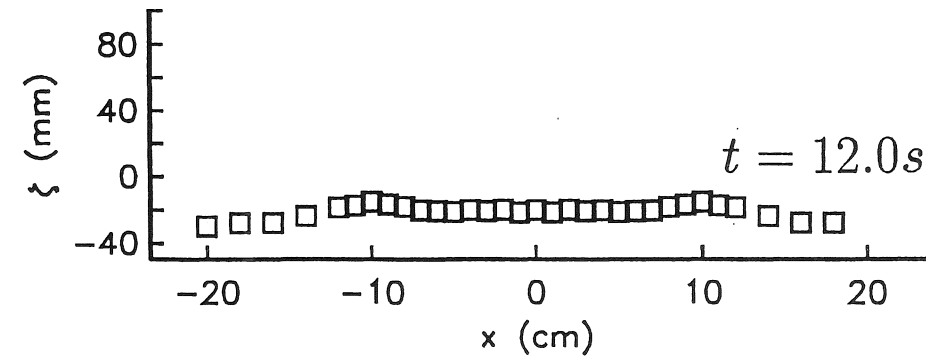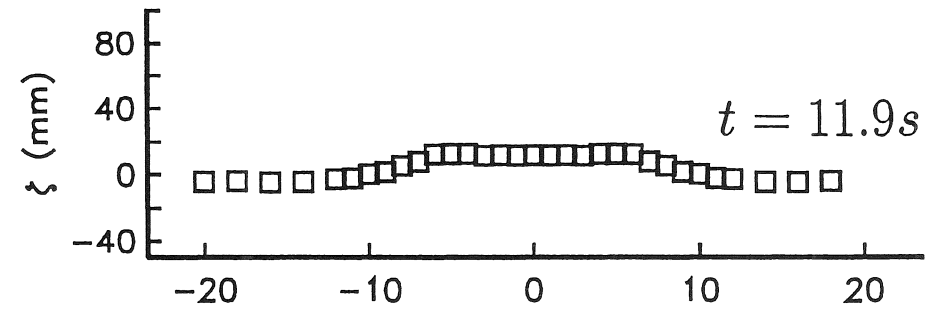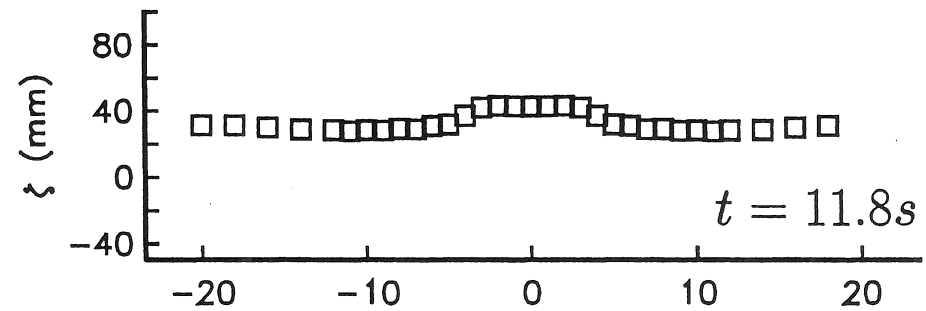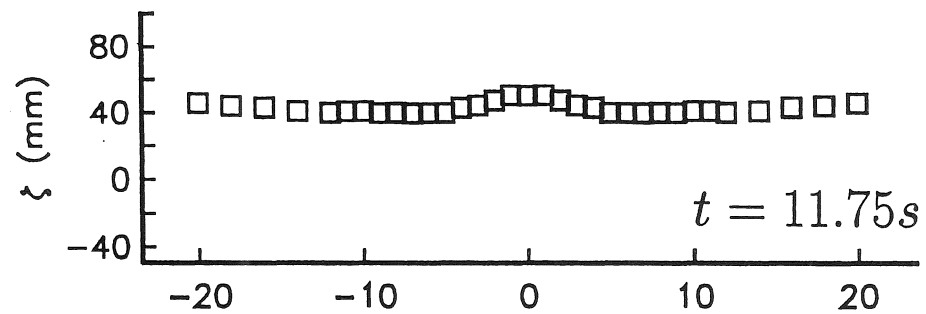
Figure 7.
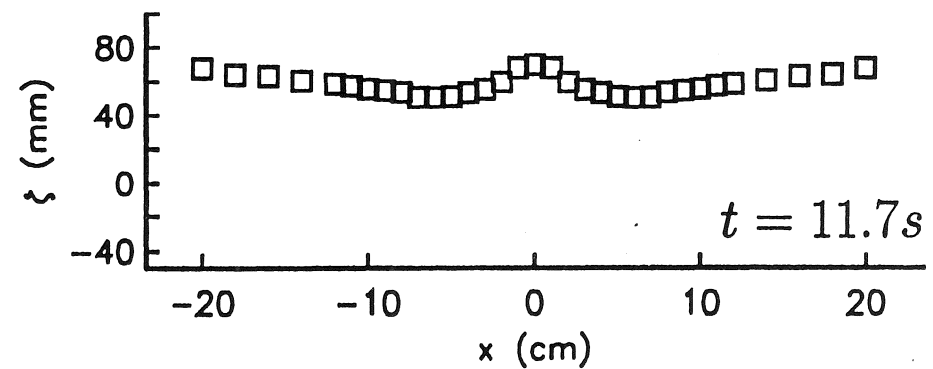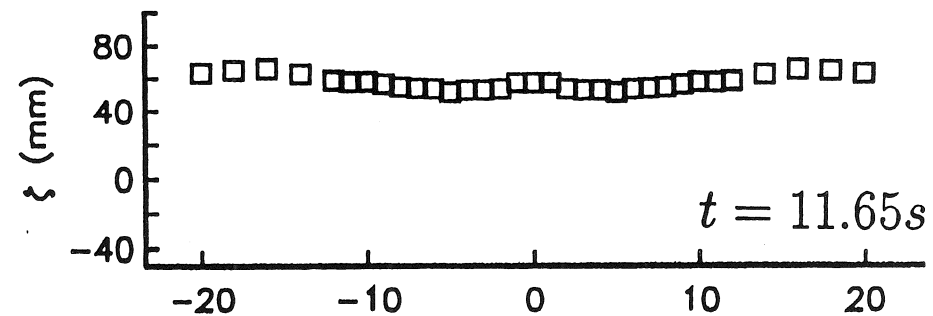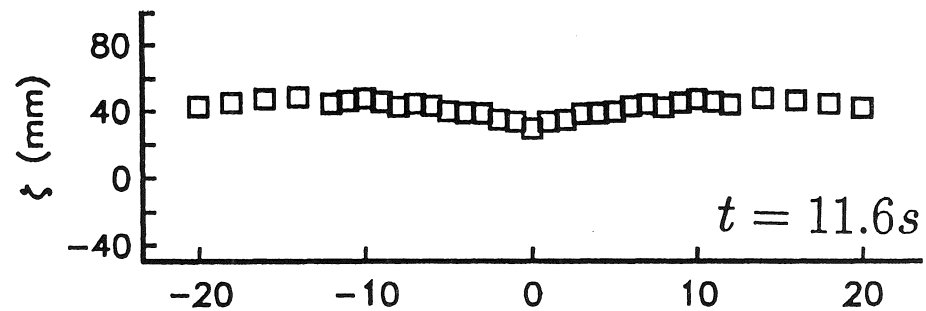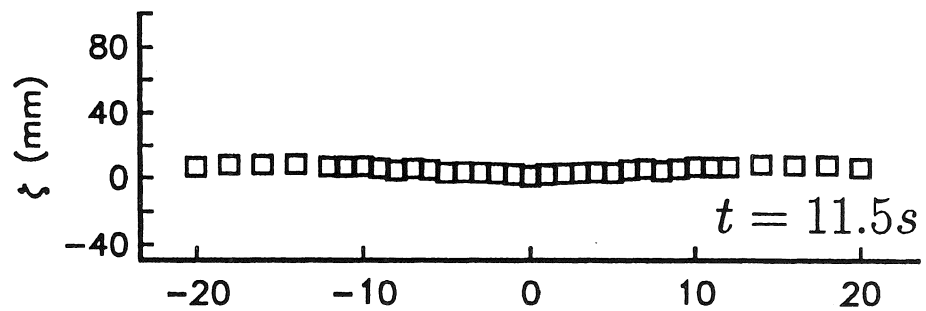
b)
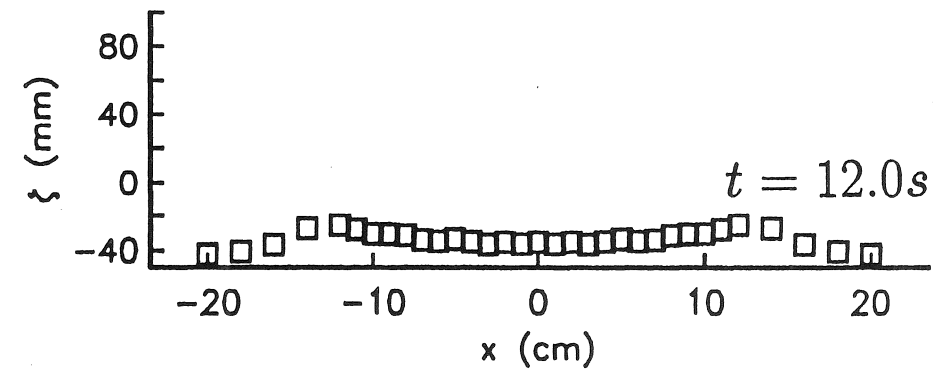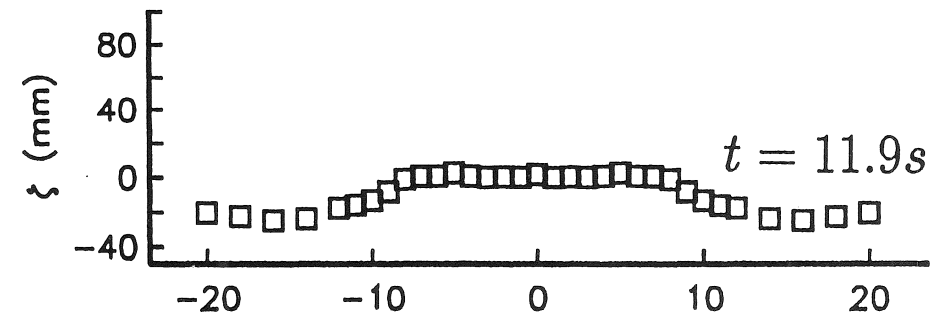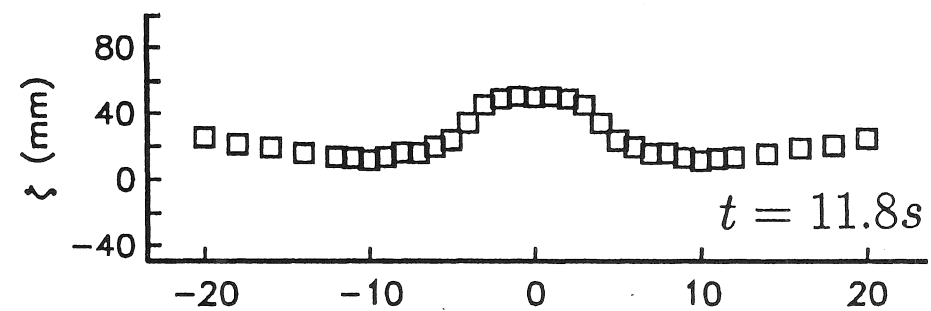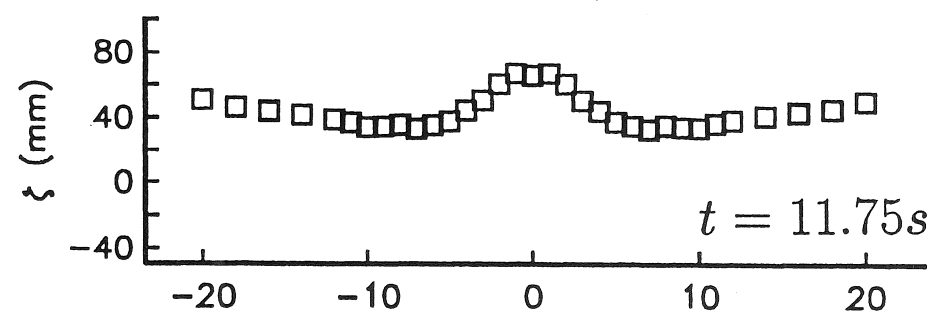
Figure 7.

c)

Figure 7.

a)

b)

c)

Figure 8.

Figure 9.